A Mechanistic Insight into Doxorubicin Adsorption on N-isopropyl Acrylamide Grafted Nanotube: Optimization Study of Loading Temperature

Reza Maleki (rezamaleki96@gmail.com)
USERN https://orcid.org/0000-0002-5169-5848
Mohammad Dahri
Shiraz University of Medical Sciences Faculty of Dentistry
Ebrahim Ghasemy
Iran University of Science and Technology
Hossein Akbarialiabad
Shiraz University of Medical Sciences Faculty of Dentistry

Research

Keywords: Temperature-responsive, Doxorubicin, Molecular Dynamics, N-isopropyl acrylamide, Hydrogel

Posted Date: October 22nd, 2020

DOI: https://doi.org/10.21203/rs.3.rs-94360/v1

A Mechanistic Insight into Doxorubicin Adsorption on N-isopropyl Acrylamide Grafted Nanotube: Optimization Study of Loading Temperature

Reza Maleki[1]; Mohammad Dahri[2,3]; Ebrahim Ghasemi[4]; Hossein Akbarialiabad[5]

1- Computational Biology and Chemistry Group (CBCG), Universal Scientific Education and Research Network (USERN), Tehran, IranPharmaceutical Nanotechnology
2- Department and Center for Nanotechnology in Drug Delivery, School of Pharmacy, Shiraz University of Medical Sciences, Shiraz, Iran
3- Student Research Committee, School of Pharmacy, Shiraz University of Medical Sciences, Shiraz, Iran
4- Nanotechnology Department, School of New Technologies, Iran University of Science and Technology, Tehran, Iran
5- Student Research Committee, School of Medicine, Shiraz University of Medical Sciences, Shiraz, Iran

*__Correspondence: Reza Maleki,__ Computational Biology and Chemistry Group (CBCG), Universal Scientific Education and Research Network (USERN), Tehran, Iran – rezamaleki96@gmail.com:

Abstract

Background: The drug development process is costly and time-consuming; hence, nowadays, enormous efforts have been established through computational studies for finding appropriate strategies, methods and solutions for enhancing the drug production and administration procedures. Hydrogels that undertake deformation upon pertinent changes in temperature have significant aptitude as drug delivery systems. These biomaterials have made a substantial impact on the development of drugs for critical diseases, especially cancer therapy. Drug loading and uptake are primary and fundamental steps of the drug development and discovery process. N-isopropyl acrylamide is a common and well-known thermo-sensitive and injectable hydrogel for the drug uptake under the lower critical solution temperature (LCST). In the current study, carbon nanotube (CNT) as a nanocarrier was modified via N-isopropyl acrylamide. On the other hand, Doxorubicin as an anti-cancer drug applied on mentionted systems to develop drug packing at three different temperatures.

Results: After computational parametrization of the system via bioinformatics software and databases, Molecular dynamics (MD) simulation was run. To this end, the detailed simulations were carried out to reveal the interaction energy, numbers of hydrogen bonds, the gyration radius, mean square displacement, and radial distribution function as well as Gibss free energy. Besides, the optimal loading temperature for doxorubicin was determined. The results achieved from simulating the polymer demonstrated a decrease in the gyration radius at a higher temperature. A decrease of gyration radius resulted in more concentrated aggregation with stronger bonds.

Conclusions: Therefore, at the higher temperature, the more stable polymer interaction and better doxorubicin loading were acquired. The smart absorption of doxorubicin onto the CNT

modified via N-iso-propyl acrylamide (NIPA) give a significant and valuable view on the future studies regarding the drug development and novel, biocompatible, and biodegradable stimuli-sensitive drug delivery system.

Keywords: Temperature-responsive; Doxorubicin; Molecular Dynamics; N-isopropyl acrylamide; Hydrogel

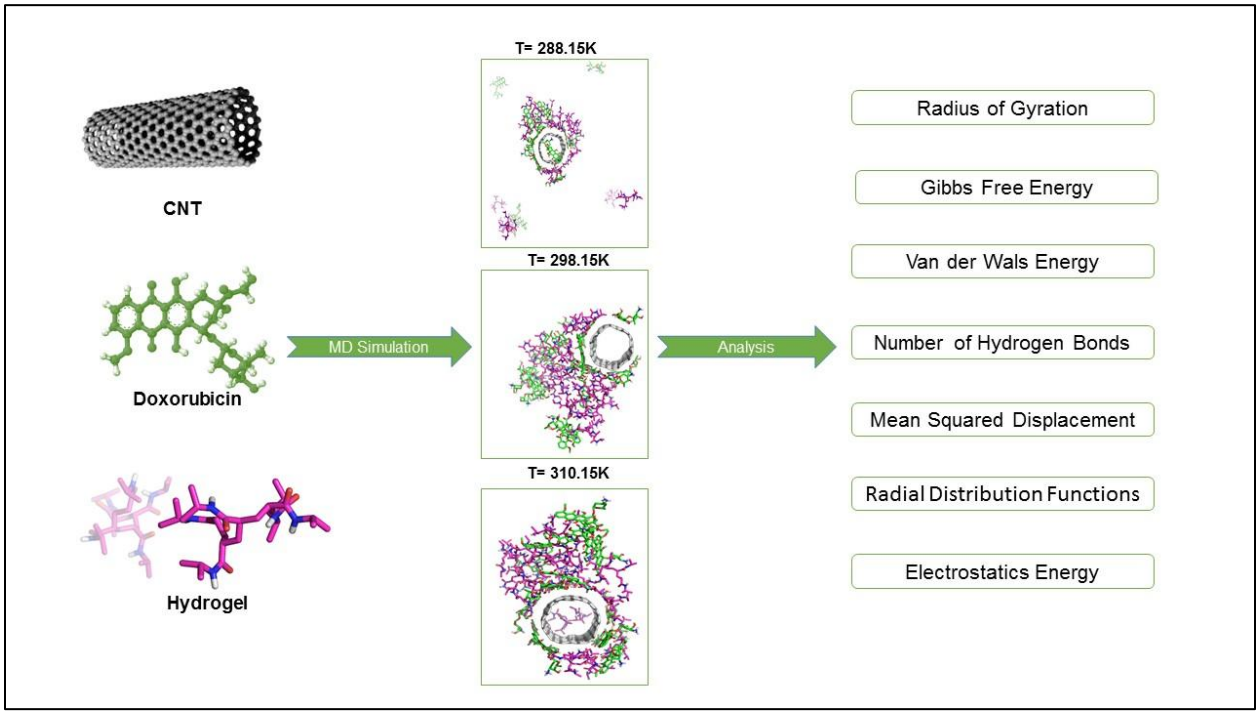

Background

Cancer is one of the global, critical and life-threatening diseases which was the third leading causal factor of death in 1990, while it rose to be the second leading cause of mortality in 2013. In 2013, around 15 million cancerous patients were identified, and cancer led to around 8.2 million deaths. In that year, statistical analysis showed that the cancer resulted in 196.3 million cancer cases (1).

Many drugs and modalities have been introduced to battle the cancerous cells. Doxorubicin (DOX) is one of the essential and common anti-cancer drugs which fights against the proliferation and metastasis of cancerous cells. DOX binds to the DNA and inhibits the nucleic acid production (2). As such, it disrupts the molecular structure as well as the spatial blockage. DOX is used to treat various cancers such as gastric, lung, breast, bladder, ovary, thyroid, bone, nerve tissue, muscles, joints, and soft tissue malignancies (3). It is also used to heal Hodgkin's lymphoma and multiple types of leukemia (4). On the contrary, the drawback of the DOX which has an adverse effect, is the fact that it can also damage healthy human cells and prevent their growth as well (5). This requires implementing novel techniques to minimize these drug-related systemic toxic effects. There are multiple methods to achieve such a goal; one of them is nanostructures which provide the targeted drug delivery. Targeted and smart drug delivery via the nanoparticles not only minimize the doxorubicin adverse and unwanted effects on the non-cancerous and healthy cells but also maximizes the efficiency of the drug on tumor cells (6).

Novel nanostructured drug delivery systems have dramatically improved drug therapies (7). Various polymeric (8), carbon-based (9), and ceramic nanostructures (10) have been studied for this purpose. These structures have specific features including targeted drug delivery (11), high

biocompatibility (12), enhancing drug viability in the bloodstream (12), controlling and decelerating the drug release (13), protecting drug molecules (14), having a smaller size than the cells (15), and the ability to cross biological barriers to deliver a drug to the targeted site (16). Therefore, nanostructures can be a suitable carrier for doxorubicin delivery. Because of the high therapeutic utility of doxorubicin in oncology and clinical fields, the DOX drug development can decrease the manufacturing cost and increase the efficacy and minimize the drawbacks (17).

Carbon nanotubes have recently received massive attention in the delivery of various drugs (18). Carbon nanotubes have an amazing ability to detect and damage cancer cells in vivo. Many researchers have focused on the potential capabilities of carbon nanotube as a carrier for anti-cancer agents that may have unique physical and chemical characteristics such as size, geometric shape, surface charge, surface chemistry, hydrophobicity, and more importantly, the ability to cross biological barriers in vivo (17, 19-22). These particles are small enough to cross the membranes and biological barriers and carry the drug into the malignant cells (23). These structures possess a high surface area which enables us to accomplish the surface engineering and change the surface properties. The carbon nanotubes can be functionalized according to the intended use with various functional groups and compounds to enhance their solubility and biocompatibility (24, 25). Drug compounds are loaded onto the surface or into the carbon nanotubes. The surface engineered nanotubes are widely used in the drug delivery (26). The nanotubes can move comfortably inside the biological membranes, skin, blood vessels, and penetrate into the biological tissues. These features have made nanotubes a useful carrier for drugs, genes, proteins, and vaccines (27, 28). For such reasons, the chemical and physical functionalizations of the nanotubes have been investigated to stabilize the functional groups in the water environment (29).

Hydrophilic polymers can stabilize nanotubes in the aquatic environment. The pH-sensitive polymers such as polyacrylic acid have been used as a carbon nanotube functional group, in which the nanotubes are dispersed in water based on the degree of polymer ionization and pH. For nanotubes, the use of temperature-sensitive polymers instead of the pH-sensitive polymers is a more suitable option in the aqueous environment. The pores in the hydrogels facilitate the loading of the drug on/into the carriers and may serve as a drug delivery system (30). The hydrogels used for drug delivery systems are used in the form of slabs, microparticles, nano particles, coatings, or films. Hydrogels are used to release both hydrophilic and hydrophobic drugs (31). Both hydrophilic and hydrophobic drugs can be simultaneously incorporated into hydrogels because hydrogels have both hydrophilic and hydrophobic groups. Hydrophobic groups interact with doxorubicin, which is hydrophobic, and hydrophilic groups interact with water. Thus, hydrogels can inhibit the accumulation of doxorubicin molecules and are attractive carriers for doxorubicin (32).

N-isopropyl acrylamide (NIPA) is one of the thermal-sensitive hydrogels and hydrogels. These polymers have a critical solution temperature in aqueous solution. The volume and shape of the NIPA are changed reversibly in the vicinity of solution temperature. There is a polymer phase transition in the water at the low critical solution temperature (LCST), whereby the polymer is transformed from a distended hydrophilic structure below the critical solution temperature to a condensed hydrophobic structure above this temperature (33).

The polymer of our current study, NIPA, is one of the conventionals, biocompatable, biodegradebale and thermo-sensitiver injectable hydrogels which are physiologically and chemicaly capatable to load and delivery Therapeutic agents. Anticancer agents are naturally

entrapped in the thermo-sensitive hydrogel by mixing with precursor solution and then after by sterilization procedure the hydrogel is capable to inject to the body biofluids (34, 35).

Other studies showed that the essential solution temperature of the NIPA could be increased by combining with carbon nanotubes (28). Other properties of the NIPA, such as the release time, can also be improved in combination with carbon nanotubes. Hydrophilicity and hydrophobicity of the NIPA can also be varied according to their composition. Multiple functional groups have been used to modify the properties of the NIPA. One of the attractive compounds for drug delivery and features of the NIPA can be the NIPA@CNT nanocomposite composite (36).

Molecular dynamics (MD) is a powerful tool that can provide qualitative and quantitative information on the Physico-chemical interactions and mechanisms of chemical and biological systems that provoide more conceptual results in comparison to machine learnin methods (37-39). Considering the difficulties and high-cost of empirical experiments, many studies have been done by MD to simulate the drug delivery systems in cancer therapy (40, 41). In previous studies, MD has been carried out for the release of the doxorubicin by carriers such as graphene and graphene oxide (42). In these studies, the effects of pH, molecular bonds, carrier size, and functional groups have been investigated (43). Previous works have not studied the drug development process during temperature changes, such as the uptake and loading mechanism of the doxorubicin by carbon nanotubes using MD (44).

Utilizing the molecular cloning, this work investigates the N-isopropyl acrylamide@CNT nanocomposite as a suitable carrier for the loading of the doxorubicin. To analyze the characteristics of this attractive carrier, the interactions between the carrier and drug, gyration radius, hydrogen bonds, and radial distribution function have been investigated. In order to peruse the effect of the polymer nano-particle synthesis temperature on the loading and drug

delivery properties, three different temperatures have been considered for isopropyl acrylamide, and three simulations have been performed for isopropyl acrylamide polymers. The comparison of results determines the optimal temperature for the drug loading.

Result and discussion

1.1. Hydrogen bond analysis

Hydrogen bonds can be formed between hydrogen atoms and high electronegative atoms (such as oxygen, nitrogen, or fluorine) as well as between various electronegative biomolecules. The H-bond analysis is one of the most well-organized indicators for comparing the ability of several structures in capturing various adsorbates. The higher number of hydrogen bonds reveal the more interactions between the biomolecules as well as the propensity for the two different or same particles to be highly attracted to each other. Hence, the number of hydrogen bonds formed between the DOX, N-isopropyl acrylamide, and CNT is an index to evaluate the drug uptake and stability of drug delivery systems at three various temperatures. The amine and carboxylic acid functional group can form hydrogen bonds; under proper conditions, the hydrogen attached to the amine or carboxylic group can create Hydrogen bonds. The N-isopropyl acrylamide possesses an N containing group, in which, the N atoms can create H-bonds. According to the presence of a Hydroxyl group in the DOX molecular structure, H-bonding is possible between the OH group and the other molecules. Regarding Figure 2, the average number of H-bonds created during the MD simulation at 288.15 K, 298.15 K, and 310.15 K temperatures were 6.01966113, 5.937687438, and 1.325558147, respectively. The higher numbers of H-bond at 288.15 K indicate the more appropriate drug loading and uptake in comparison with two other temperatures. However, this analysis alone is not sufficient to evaluate the interactions between

molecules, so we studied the other bond interactions between the drug, hydrogel, and nanocarrier.

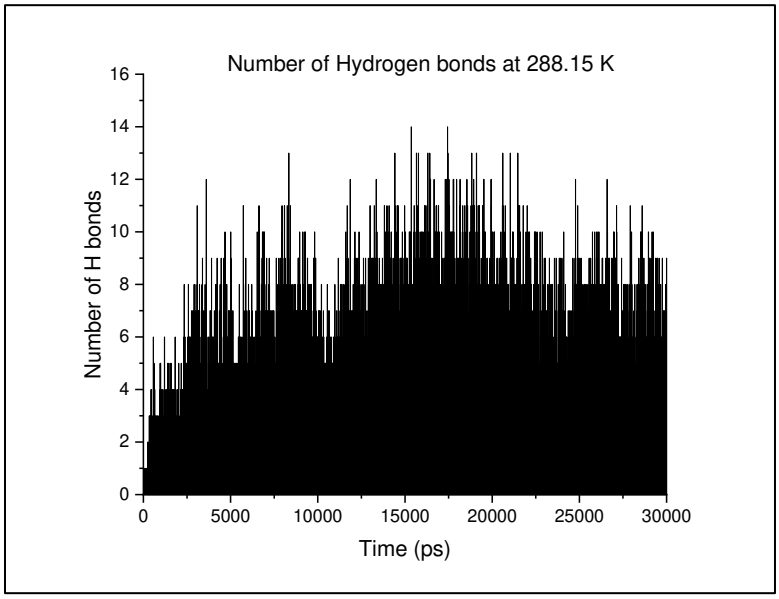

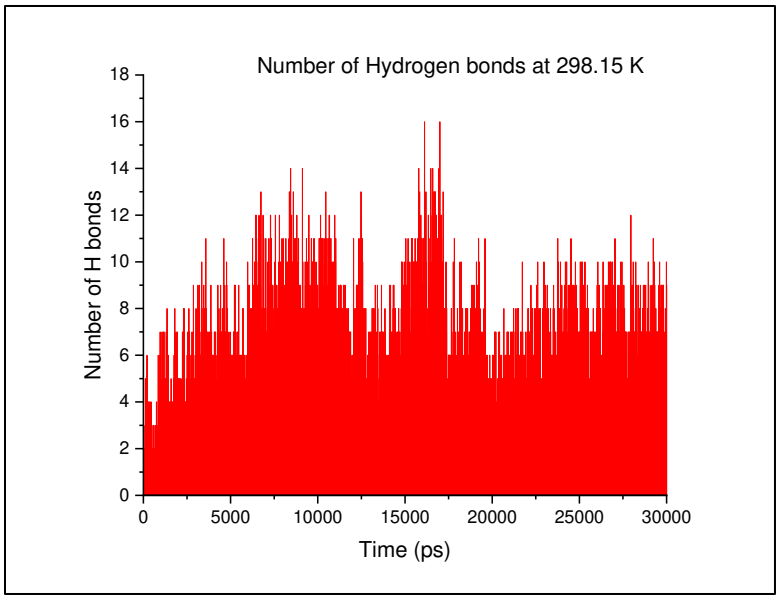

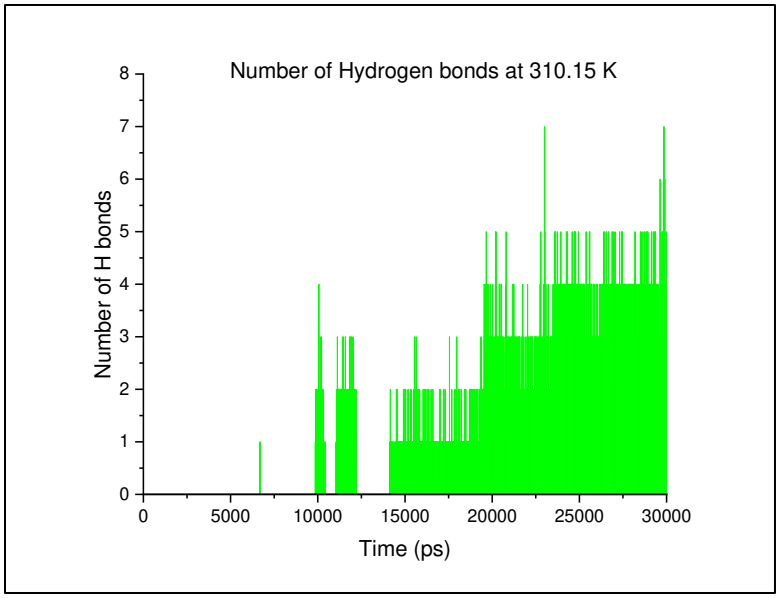

Figure 2. The numbers of hydrogen bonds between DOX and NIPA at three different temperatures

1.2. Interactions of energy analysis at three different temperature

Figures 3, 4, and 5 demonstrate the DOX@CNT / DOX@NIPA / NIPA@CNT interactions at three different temperatures including 288.15 K, 298.15 K, and 310.15 K. The diagrams (a), (b) and (c) illustrate the van der Waals and Electrostatic interaction energies. According to these curves, the total interaction energies at 310.15 K are higher than others. This fact would assist in the adsorption of the DOX. It can be inferred that the temperature of 310.15K is an optimal temperature for the DOX loading onto the surface of the CNT.

In both interaction diagrams, the electrostatic energy is lower and near to zero. This can be attributed to the absence of the charge for the drug, polymer, and nanocarrier. While the van der Waals interaction is noticeable , so dominant interaction energy of total is related to recent energy. The total interaction energy between the DOX and PIN at 310.15 K and 298.15 K were almost the same while the energy at 288.10 K was the lowest. These curves also indicate that the

electrostatic energy has no role in the DOX@CNT and NIPA@CNT interactions at different temperatures, in which the total energy was almost equal to the van der Waals energy. This can be ascribed to the Aromatic groups of the DOX molecules, which can establish significant van der Waals interactions with the non-polar functional groups of the CNT and NIPA molecules at different temperatures.

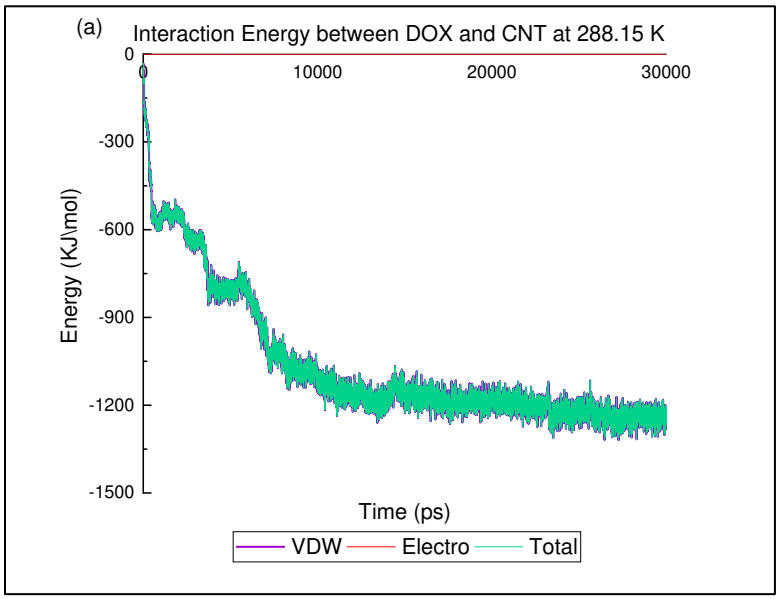

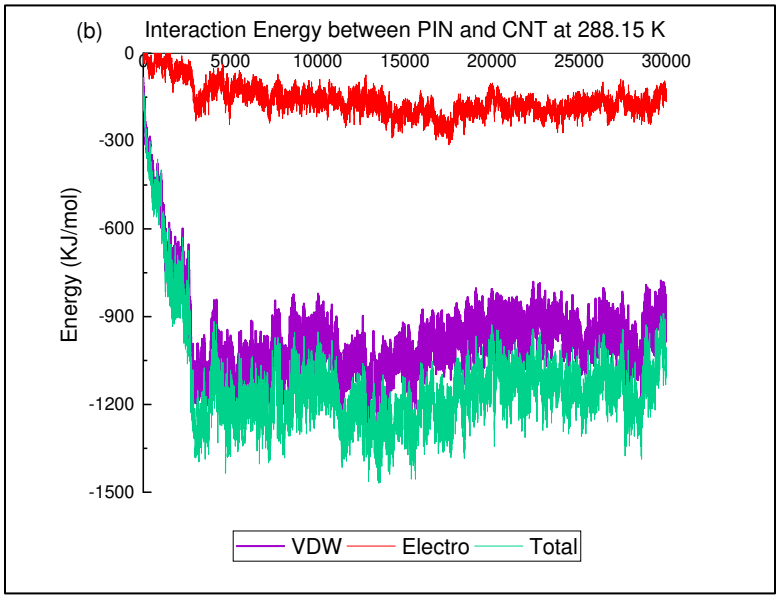

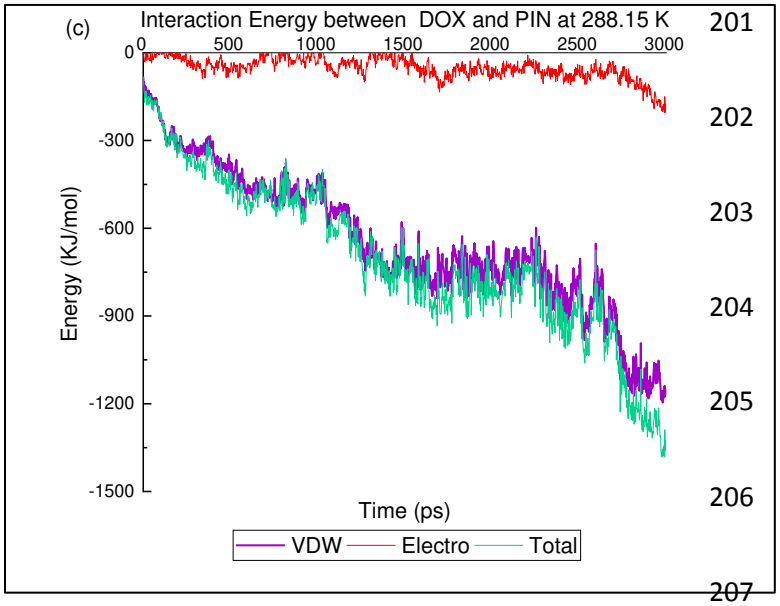

Figure 3. Interaction energies diagrams at 288.15 K

(a) Electrostatic and van der Waals energies of DOX@CNT interaction versus time at 288.15 K;

(b) Electrostatic and van der Waals energies of NIPA@CNT interaction versus time at 288.15 K;

(c) Electrostatic and van der Waals energies of DOX@NIPA interaction versus time in 288.15 K

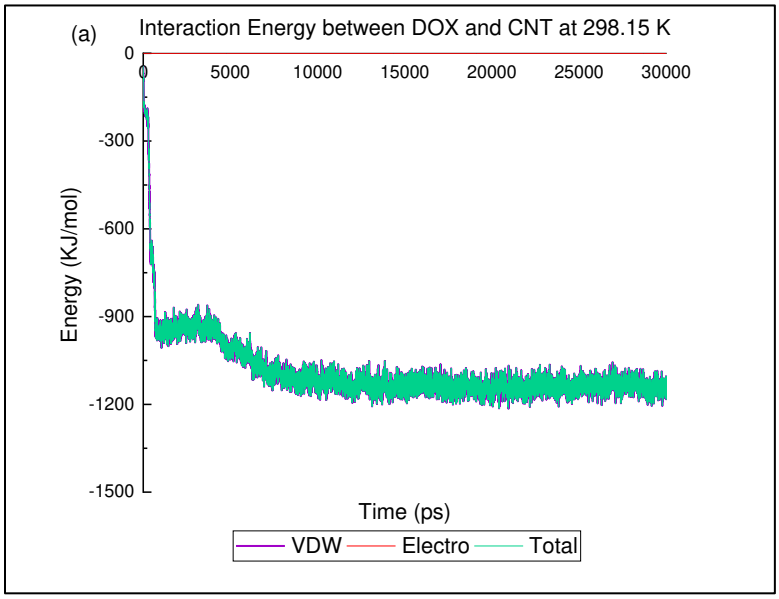

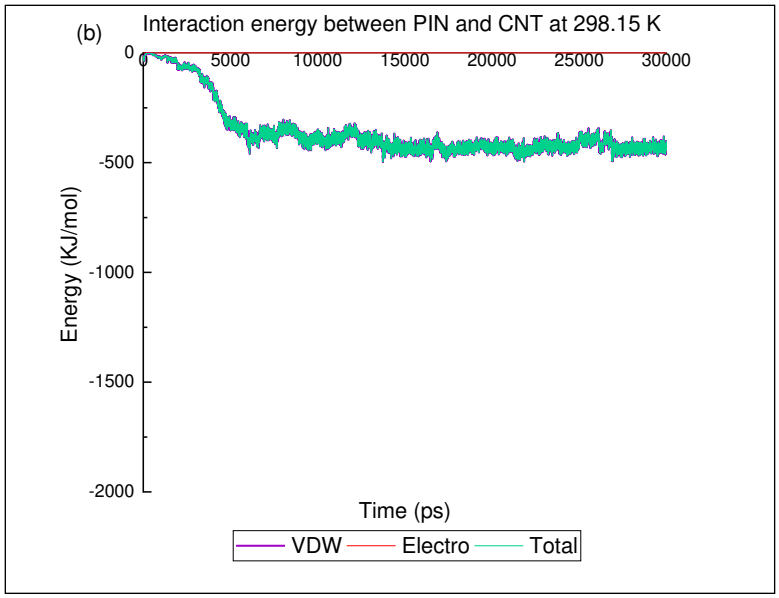

213

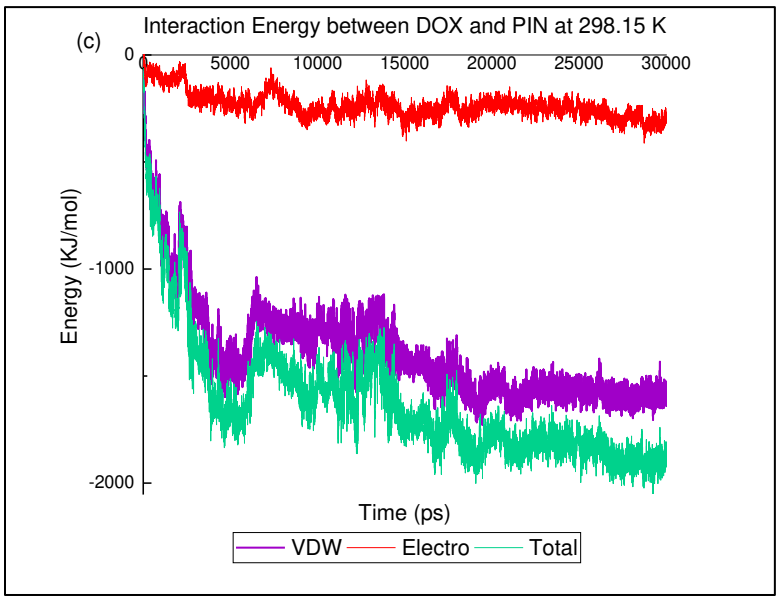

214

215 **Figure 4.** Interaction energies diagrams at 298.15 K

216 (a) Electrostatic and van der Waals energies of DOX@CNT interaction versus time at 298.15 K;

217 (b) Electrostatic and van der Waals energies of NIPA@CNT interaction versus time at 298.15 K;

218 (c) Electrostatic and van der Waals energies of DOX@NIPA interaction versus time in 298.15 K.

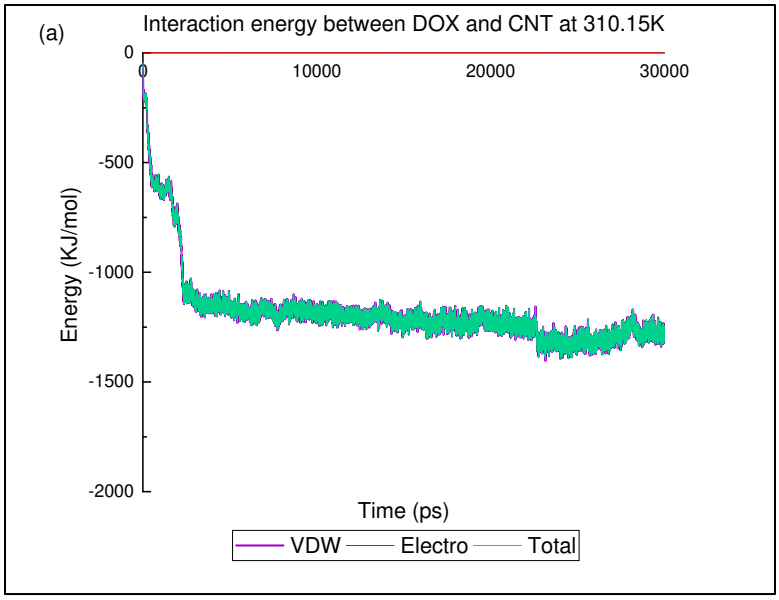
(a)
Interaction energy between DOX and CNT at 310.15K
0
-500
-1000
-1500
-2000
0
10000
20000
30000
Energy (KJ/mol)
Time (ps)
VDW
Electro
Total

219

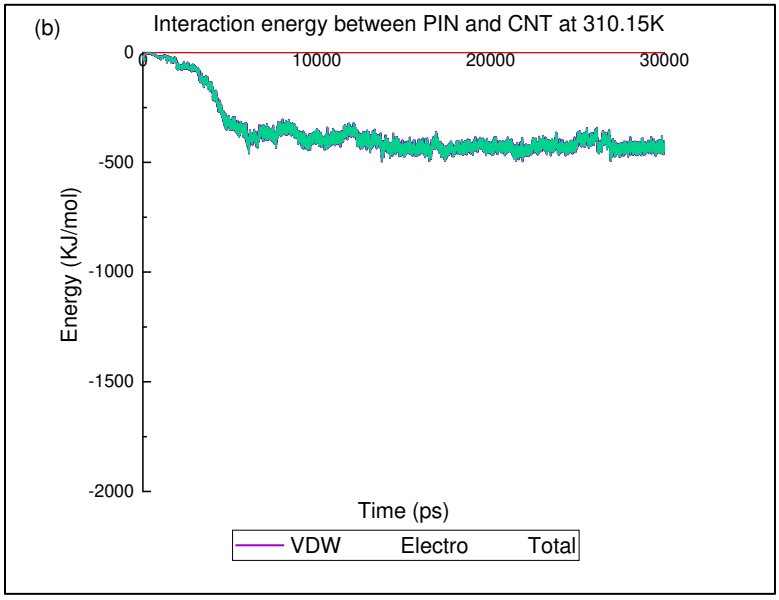
(b)
Interaction energy between PIN and CNT at 310.15K
0
-500
-1000
-1500
-2000
0
10000
20000
30000
Energy (KJ/mol)
Time (ps)
VDW
Electro
Total

220

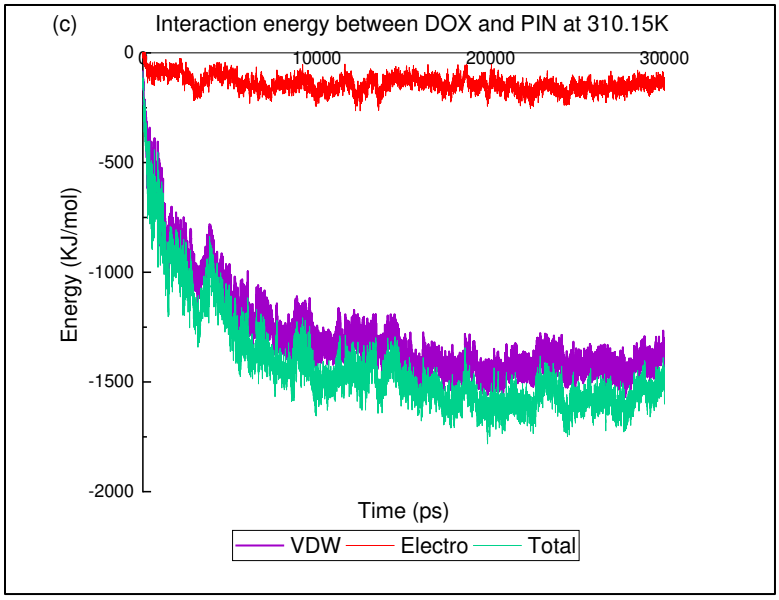

Figure 5. Interaction energies diagrams at 310.15 K

(a) Electrostatic and van der Waals energies of DOX@CNT interaction versus time at 310.15 K;

(b) Electrostatic and van der Waals energies of NIPA@CNT interaction versus time at 310.15 K

(c) Electrostatic and van der Waals energies of DOX@NIPA interaction versus time in 310.15 K.

1.3. Radius of Gyration

Gyration radius (Rg) is a factor by which the accumulation of molecules (such as hydrogels) and alteration of bio-macromolecule size (nucleic acids) can be computed and evaluated. The higher the gyration radius, the stronger the aggregation of the DOX@NIPA, and thus the conjugation would be of a more stability. Figure 6 shows the gyration radius of the DOX and NIPA for the CNT carriers. At different temperatures, the gyration radius of the interacting particles for NIPA and DOX was in a similar order, while at 310.15 K the lower Rg indicated the better stability.

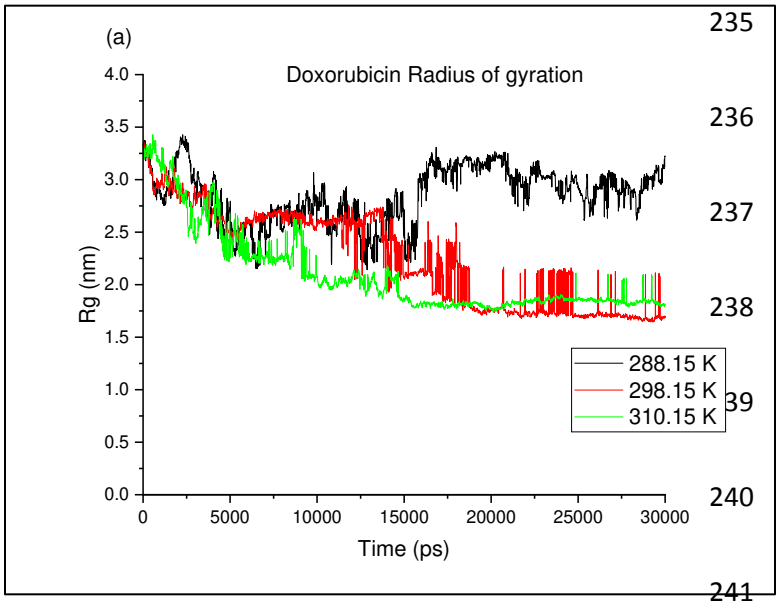

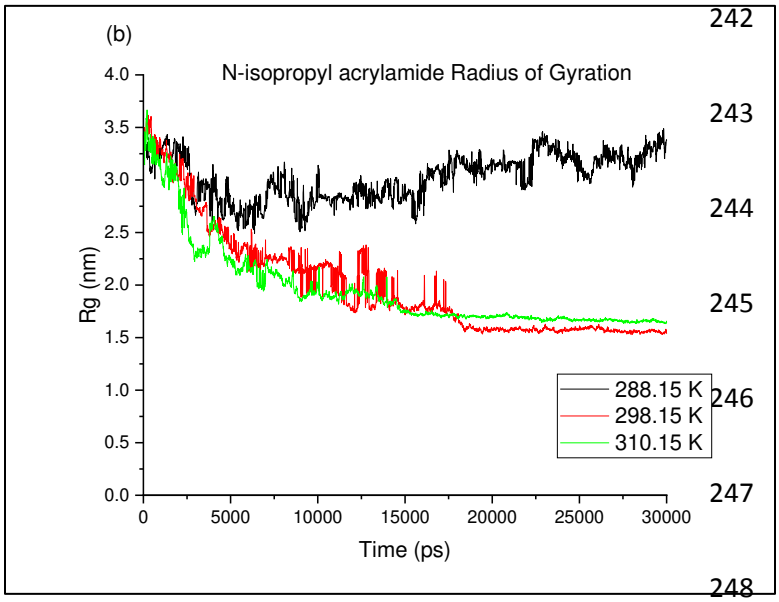

Figure 6. Gyration Radius of Molecules versus time in different temperatures for CNT carrier: (a) DOX Rg at three temperatures (b) NIPA Rg at three temperatures

1.4. Mean Square Displacement Analysis

The mean displacement square (MSD) is a computational factor to estimate the drug diffusion coefficient. The situation of all atoms is denoted by 'r', while 't' signifies the time. The

following formula indicates how the mean square displacement is obtained:

$$MSD = \langle [r(t) - r(0)]^2 \rangle = \frac{1}{t} \sum_{t=t_0}^{t} [r(t) - r(0)]^2 \quad (3)$$

Einstein's relation reveals how the diffusion coefficient for the three-dimensional system can be calculated.

$$D = \frac{1}{6} \frac{MSD}{t} \quad (4)$$

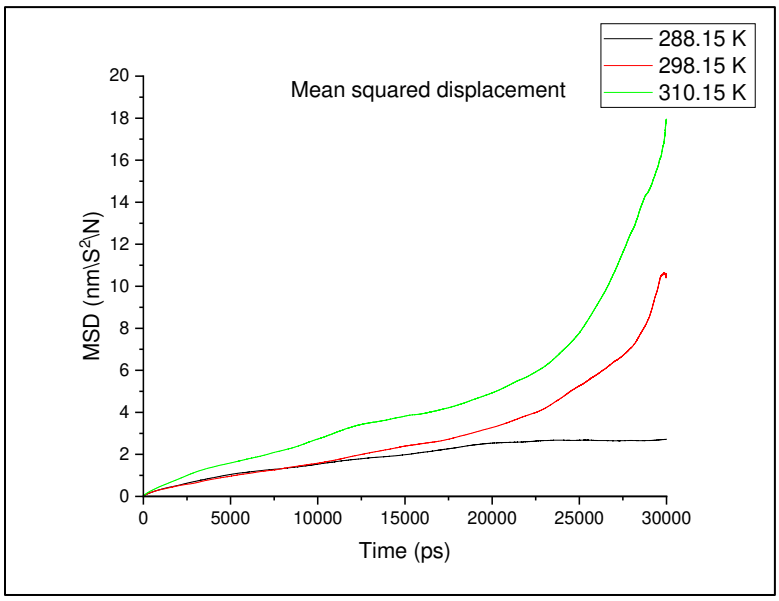

Figure 7. Mean square displacement of the system versus time at different temperature

In Figure 7, the vertical axis represents the MSD and the horizontal axis indicates the time in picoseconds. According to the mentioned equation, the slope of the MSD curve demonstrates the diffusion coefficient, and the higher the slope of the graph, the higher the diffusion coefficient. The comparison of the figures reveals that at 310.15 K, the chart has a higher slope. Therefore, at 310.15 K, the diffusion coefficient was more significant. The higher diffusion coefficient means that the drug is absorbed more rapidly ovo the surface of the CNT and the hydrogel; accordingly, the efficiency and rate of the drug absorption will be higher. So, the drug loading takes place

excellently at 310.15 K, and this temperature is better for loading the doxorubicin onto the nanotube-polymer carrier.

1.5. Radial Distribution Function analysis

Figure 8 (a) shows the radial distribution function (RDF) of the DOX's in interaction with the CNT. The vertical axis represents the RDF value, and the horizontal axis indicates the location of the molecules. As mentioned earlier, at any point where the RDF is higher, the molecule accumulates at that point. It is clear from the figure that all curves have a maximum point where the RDF value is maximum, and at that point, there is a more significant accumulation of molecules. The temperature of 310.15 K has a higher peak point than other temperatures. As a result, the optimal temperature for both the accumulation of doxorubicin on the CNT and its absorption is 310.15 K. (Figure 8 a). Moreover, the RDF of the polymer in connection with the CNT is demonstrated in Figure 8 b. Three curves are visible in the graph corresponding to three temperatures of 288.15 K, 298.15 K, and 310.15 K. The RDF curve for each temperature has a maximum point. At the maximum point, the accumulation of molecules is more significant than elsewhere in the simulation box. The RDF curve at 310.15 K had a higher peak point than other temperatures, so there is more molecular accumulation at this temperature than other temperatures. The polymers are better assembled around a point at 310.15 K and form a more stable structure. Therefore, it can be concluded that 310.15 K is a temperature better for the accumulation of polymers around the carbon nanotube in comparison to the 288.15 and 298.15 K temperatures.

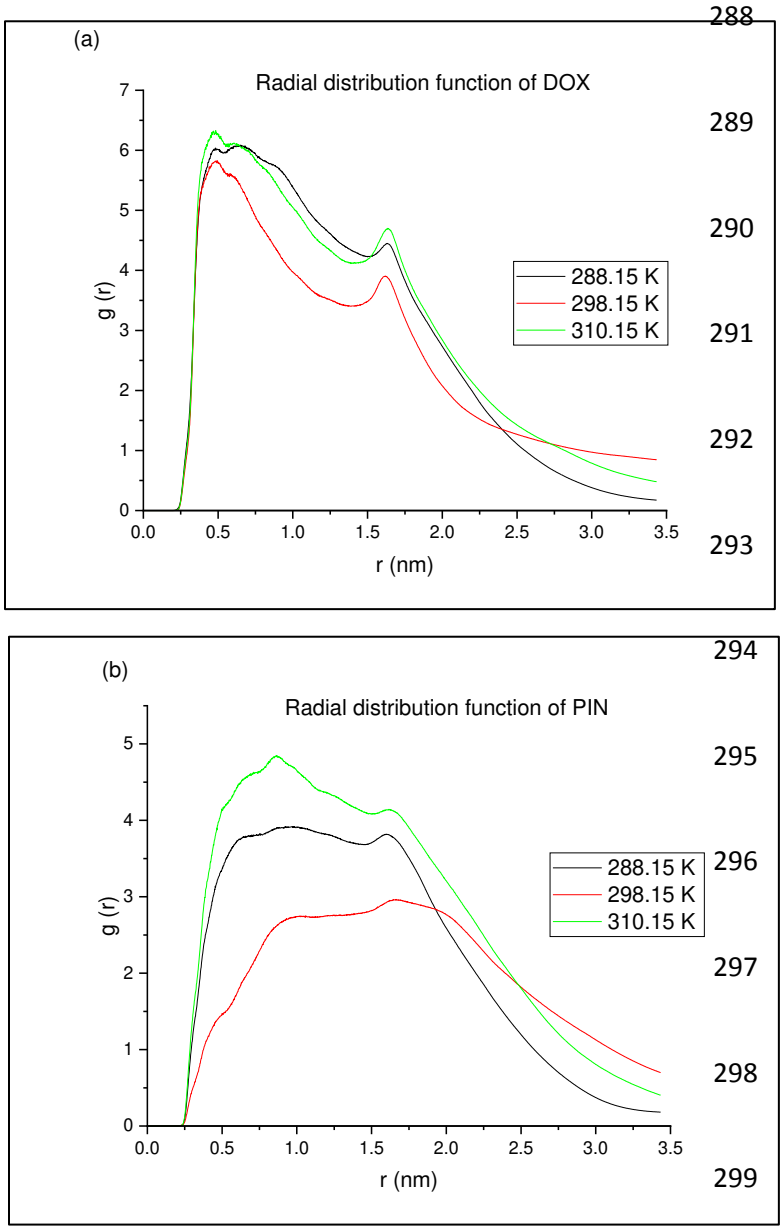

Figure 8. The radial distribution function of the DOX@CNT and NIPA@CNT versus location at different temperatures: (a) The RDF of the DOX at three temperatures; and (b) the RDF of the NIPA at three temperatures.

Conclusion

In recent decades, development of biomaterials, especially drug delivery and tissue engineering systems, has increased the quality and selectivity of the medical products in patients. Poly (n-isopropyl acrylamide) as a thermo-responsive polymeric nanoparticle has a significant role in smart drug delivery systems. In this work, the loading of doxorubicin on the carbon nanotube and Poly (n-isopropyl acrylamide) as a thermo-sensitive polymer, was simulated at three variouse temperatures, and the effect of the temperature on drug loading and packaging was investigated. Utilizing Gromacs software the molecular dynamics factors including. the gyration radius, hydrogen bonding, mean square displacement as well as radial distribution functions was calculated. This study, provided a molecular and atomistic insight into the doxorubicin, Poly (n-isopropyl acrylamide), and carbon nanotube interaction which is a prerequisite of developing novel nanomedicine systems for pre experimental drug development studies. Particularly, simulation results indicated that the drug loading at 298.15K and 310.15K have stronger interaction in comparsion with 288.15K. This result is related to percence of injectable and thermo-sensitive hydrogel in delivery systems. Furthermore, According to Gibss energy calculation,……so the ……..temprature is appropriate value for loading of dox. For the subsequent studies, researchers could investigate the condition of the Physico-chemical properties of DOX/NIPA@CNT.

Materials and Methods

1- Molecular dynamics

Gromacs version 5.1.2 software was used to perform the simulation. Ambertools software was used to obtain the polymer optimum parameters. The OPLS-aa force field was used and the TIP3P water model was adopted as the solvent. Parameters of Ambertools were converted to Gromacs using the ACPYPE script.

The parameters analyzed in these simulations are:

1- The gyration radius or aggregation of polymer molecules at one point

2- The number of hydrogen bonds between the polymer/polymer, polymer/drug, polymer/nanotube, and drug/nanotube

3- The van der Waals energy between the polymer-polymer, polymer-drug, polymer-nanotube, and drug-nanotube

4- The mean displacement square at three various temperatures

5- The radial distribution function of the polymer, drug, and nanocarrier

In this simulation, we will label the polymer as NIPA, the drug as DOX, and the nanotube as CNT. Calculations and simulations were performed using the Gromacs software, and all images and charts were provided using the VMD® 1.9.3 and OriginLab® software.

The gyration radius can indicate the interactions between the polymer chains and solvent molecules. Gyration radius is a parameter that can be used to analyze the accumulation or aggregation of the molecules such as polymers and resize biological macromolecules such as proteins and nucleic acids over time. The gyration radius is obtained from the following formula:

$$R_g^2 = \frac{1}{2N^2}\sum_{i,j} \left(r_i - r_j\right)^2 \qquad (1)$$

where, 'N' is the number of monomers, and 'r' is the location vector of each monomer.

Radial distribution function (RDF) was used to compare the drug molecules distribution around the polymer and to calculate the aggregation of drug molecules and drug-polymer diffusion. The drug-polymer radial distribution function is the probability of finding an atom of the drug molecule at a radial distance 'r' from an atom of the polymer molecule.

Moreover, the RDF of the drug-drug is the probability of finding one atom of the drug molecule at a radial distance from an atom of the drug molecule. The general formula for the radial distribution function is as follows:

$$g_{AB}(r) = \frac{\rho_{B(r)}}{\rho_{B\,(local)}} \qquad (2)$$

In this equation, 'ρ' is the density of the particle at 'r' distance.

Figure 1 shows a three-dimensional schematic of the 5-mer, 10-mer, and 15-mer polymer molecules of the N-isopropyl acrylamide.

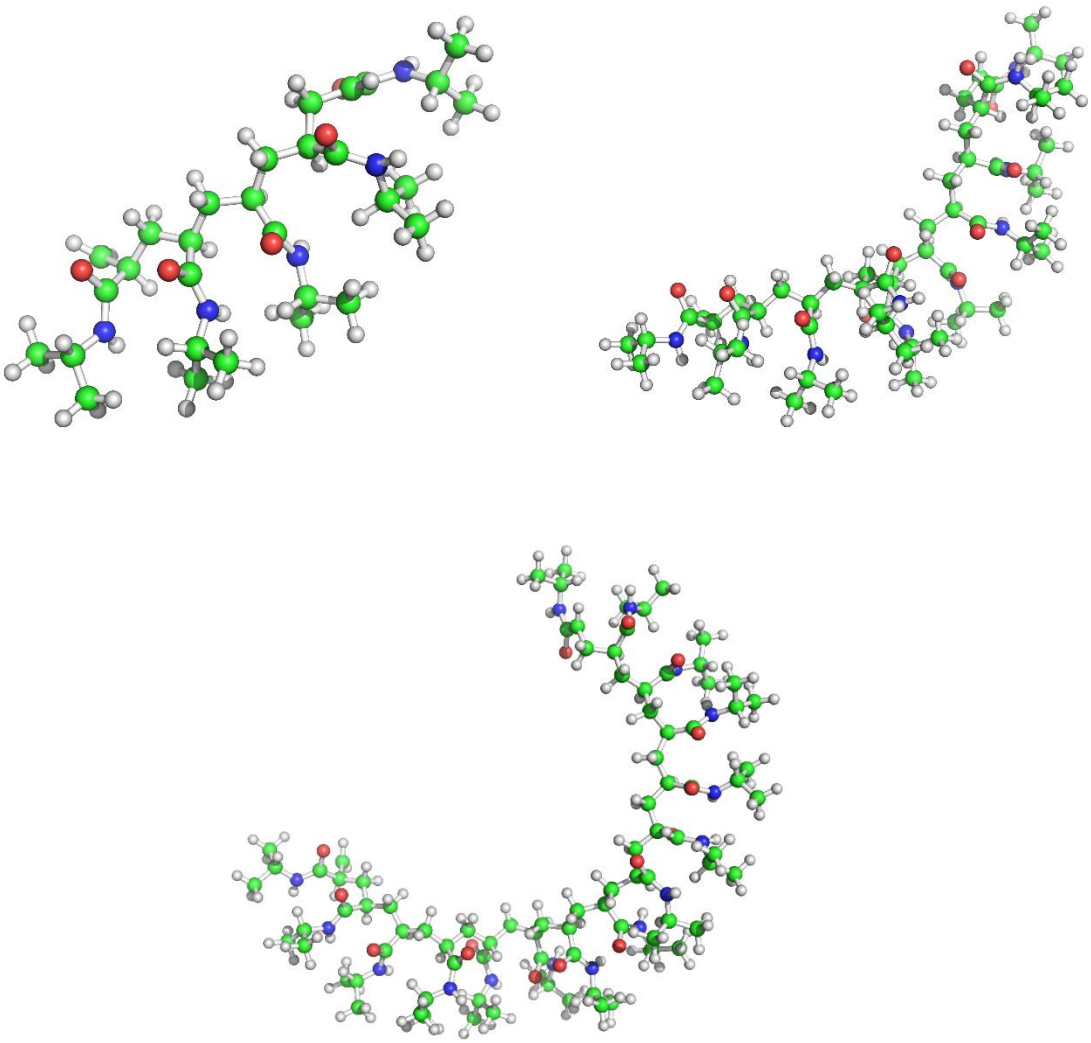

Figure 1. The 3D image of the 5-mer, 10-mer, and 15-mer polymer

Table 1: Surface charge of polymer atoms with single mer

Atom	BCC	Σ
C1	-0.23	0.34
H8	0.08	0.265

H9	0.08	0.265
H10	0.08	0.265
C	0.021	0.34
C2	-0.23	0.34
H5	0.08	0.265
H6	0.08	0.265
H7	0.08	0.265
H1	0.13	0.247
N	-0.381	0.325
H	0.219	0.107
C3	0.335	0.34
O	-0.379	0.296
C4	-0.22	0.34
H2	0.128	0.26
C5	-0.133	0.34
H3	0.129	0.26
H4	0.129	0.26

There are noticeable Hydrogen bonds and electrostatic interactions between the drug and N-isopropyl acrylamide. Therefore, measuring the surface charges of the system is very important. One popular and appropriate mathematical method to precisely calculate the surface charge in quantum mechanics (QM) is the Bond Charge Correction (BCC) method. Table 1 shows the monomer parameters in the polymer according to the surface charge correction method.

2- Structure preparation

The crystal structures of the DOX were obtained from the DrugBank database (Accession Number: DB00997). By employing the Avogadro and Gaussian software, the NIP structural topology and structure were determined and optimized. The CNT structure was designed with Nanotube Modeler 1.7.9 software.

3- Molecular dynamics simulation

In this study, N-isopropyl acrylamide polymer (NIPA) was used in the presence of CNT to investigate the uptake and loading of the doxorubicin as an anticancer agent. According to our previous study (41), polymer sizes were selected for simulation in three modes:

1- A polymer with five subunits length (15 polymers of 5-unit polymers were used in this simulation, and the total number in the simulation box was 75).
2- A Polymer with 10 mer lengths (8 number of 10-unit polymers were used in this simulation)
3- A Polymer with 15 mer length (5 polymers of 15-unit polymers were used in this simulation)

The number of simulations was three and the duration was 30 nanoseconds. In the first simulation, 15 5-unit polymers with five drugs and one nanotube were used. In the second

simulation, eight polymers of 10 units with five drugs and one nanotube were used and in the third simulation, five polymers of 15 units with five drugs and one nanotube were used. As reported in our last study, the optimum length of the NIPA chains was obtained to be 5-mer hydrogel; hence, we developed this polymer for our current study to investigate the DOX loading. In particular, three different temperatures including 288.15 K, 298.15 K, and 310.15 K were assumed as the critical points and the loading of drugs was developed at these three temperatures. Furthermore, by applying the Umbrella Sampling simulation method, we calculated the Gibbs free energy of the system during our MD simulations.

List of abbreviations

Abbreviations	**Full form**
CNT	Carbon nanotube
NIPA	N-isopropyl Acrylamide
DOX	Doxorubicin
Fig	Figure
GROMACS	Groningen machine for chemical simulations
OPLS-aa	Optimized Potentials for Liquid Simulations-all atom
MD	Molecular dynamics
Rg	Radius of Gyration
BCC	Bond Charge Correction
QM	quantum mechanics
RDF	radial distribution function
ACPYPE	AnteChamber Python Parser interface
MSD	Mean square displacement

LCST	low critical solution temperature

Declarations

Ethics approval and consent to participate

Not applicable

Consent for publication

Not applicable

Availability of data and materials

The datasets used and/or analysed during the current study are available from the corresponding author on reasonable request.

Competing interests

The authors declare that they have no competing interests

Funding

This research received no external funding

Author Contributions

Reza Maleki and Mohammad Dahri: conceptualization, methodology, software, analysis, visualization, data curation .Hossein Akbarialiabad: conceptualization and writing the original draft. Amirhossein Hasanpoor & Ebrahim Gasemi: supervision, writing, review, and editing

References

1. Fitzmaurice C, Dicker D, Pain A, Hamavid H, Moradi-Lakeh M, MacIntyre MF, et al. The global burden of cancer 2013. JAMA oncology. 2015;1(4):505-27.
2. Wang J, Li N, Cao L, Gao C, Zhang Y, Shuai Q, et al. DOX-loaded peptide dendritic copolymer nanoparticles for combating multidrug resistance by regulating the lysosomal pathway of apoptosis in breast cancer cells. Journal of Materials Chemistry B. 2020.
3. Szebeni J, Fülöp T, Dézsi L, Metselaar B, Storm G. Liposomal doxorubicin: the good, the bad and the not-so-ugly. Journal of drug targeting. 2016;24(9):765-7.

4. Rodday AM, Hahn T, Kumar AJ, Lindenauer PK, Friedberg JW, Evens AM, et al. First-line treatment in older patients with Hodgkin lymphoma: a Surveillance, Epidemiology, and End Results (SEER)-Medicare population-based study. British Journal of Haematology. 2020.
5. Ansari L, Shiehzadeh F, Taherzadeh Z, Nikoofal-Sahlabadi S, Momtazi-Borojeni A, Sahebkar A, et al. The most prevalent side effects of pegylated liposomal doxorubicin monotherapy in women with metastatic breast cancer: a systematic review of clinical trials. Cancer gene therapy. 2017;24(5):189-93.
6. Li J, Zhang Y, Cai C, Rong X, Shao M, Li J, et al. Collaborative assembly of doxorubicin and galactosyl diblock glycopolymers for targeted drug delivery of hepatocellular carcinoma. Biomaterials Science. 2020;8(1):189-200.
7. Ghosh A, Islam MS, Saha SC. Targeted drug delivery of magnetic nano-particle in the specific lung region. Computation. 2020;8(1):10.
8. Zhao Y, Alakhova DY, Zhao X, Band V, Batrakova EV, Kabanov AV. Eradication of cancer stem cells in triple negative breast cancer using doxorubicin/pluronic polymeric micelles. Nanomedicine: Nanotechnology, Biology and Medicine. 2020;24:102124.
9. Li J, Li M, Tian L, Qiu Y, Yu Q, Wang X, et al. Facile Strategy by Hyaluronic Acid Functional Carbon Dot-Doxorubicin Nanoparticles for CD44 Targeted Drug Delivery and Enhanced Breast Cancer Therapy. International Journal of Pharmaceutics. 2020:119122.
10. Paul W, Sharma CP. Inorganic nanoparticles for targeted drug delivery. Biointegration of Medical Implant Materials: Elsevier; 2020. p. 333-73.
11. Shaghaghi B, Khoee S, Bonakdar S. Preparation of multifunctional Janus nanoparticles on the basis of SPIONs as targeted drug delivery system. International journal of pharmaceutics. 2019;559:1-12.
12. Sun Y, Liang Y, Dai W, He B, Zhang H, Wang X, et al. Peptide–drug conjugate-based nanocombination actualizes breast cancer treatment by maytansinoid and photothermia with the assistance of fluorescent and photoacoustic images. Nano letters. 2019;19(5):3229-37.
13. Iturrioz-Rodríguez N, Correa-Duarte MA, Fanarraga ML. Controlled drug delivery systems for cancer based on mesoporous silica nanoparticles. International journal of nanomedicine. 2019;14:3389.
14. Xu C, Lei C, Yu C. Mesoporous silica nanoparticles for protein protection and delivery. Frontiers in chemistry. 2019;7:290.
15. Pinto AM, Gonçalves C, Sousa DM, Ferreira AR, Moreira JA, Gonçalves IC, et al. Smaller particle size and higher oxidation improves biocompatibility of graphene-based materials. Carbon. 2016;99:318-29.
16. Zou D, Wang W, Lei D, Yin Y, Ren P, Chen J, et al. Penetration of blood–brain barrier and antitumor activity and nerve repair in glioma by doxorubicin-loaded monosialoganglioside micelles system. International journal of nanomedicine. 2017;12:4879.
17. Cagel M, Grotz E, Bernabeu E, Moretton MA, Chiappetta DA. Doxorubicin: nanotechnological overviews from bench to bedside. Drug discovery today. 2017;22(2):270-81.
18. O'connell MJ. Carbon nanotubes: properties and applications: CRC press; 2018.
19. Karthika V, Kaleeswarran P, Gopinath K, Arumugam A, Govindarajan M, Alharbi NS, et al. Biocompatible properties of nano-drug carriers using TiO2-Au embedded on multiwall carbon nanotubes for targeted drug delivery. Materials Science and Engineering: C. 2018;90:589-601.
20. Mehra NK, Palakurthi S. Interactions between carbon nanotubes and bioactives: a drug delivery perspective. Drug Discovery Today. 2016;21(4):585-97.
21. He H, Xiao D, Pham-Huy LA, Dramou P, Pham-Huy C. Carbon nanotubes used as nanocarriers in drug and biomolecule delivery. Drug Delivery Approaches and Nanosystems, Volume 1: Apple Academic Press; 2017. p. 163-212.
22. Hasnain MS, Ahmad SA, Hoda MN, Rishishwar S, Rishishwar P, Nayak AK. Stimuli-responsive carbon nanotubes for targeted drug delivery. Stimuli Responsive Polymeric Nanocarriers for Drug Delivery Applications: Elsevier; 2019. p. 321-44.

23. Syrgiannis Z, Trautwein G, Calvaresi M, Modugno G, Zerbetto F, Carraro M, et al. Controlling Size-Dispersion of Single Walled Carbon Nanotubes by Interaction with Polyoxometalates Armed with a Tryptophan Tweezer. European Journal of Inorganic Chemistry. 2019;2019(3-4):374-9.
24. Shen Z, Wu J, Yu Y, Liu S, Jiang W, Nurmamat H, et al. Comparison of cytotoxicity and membrane efflux pump inhibition in HepG2 cells induced by single-walled carbon nanotubes with different length and functional groups. Scientific reports. 2019;9(1):1-9.
25. Hagiwara M, Kida T, Matsuda K, Kyakuno H, Maniwa Y, Honda Z, et al. Magnetic Properties of One-and Two-Dimensional Functional Materials: Oxygen Molecules Encapsulated in Single-Walled Carbon Nanotubes and Copper Ions Embedded into Phthalocyanine Sheets. The Open Chemistry Journal. 2019;6(1).
26. Zaheed M, Wilcken N, Willson ML, O'Connell DL, Goodwin A. Sequencing of anthracyclines and taxanes in neoadjuvant and adjuvant therapy for early breast cancer. Cochrane Database of Systematic Reviews. 2019(2).
27. Zhang C, Zheng Y-Y, Gong Y-M, Zhao Z, Guo Z-R, Jia Y-J, et al. Evaluation of immune response and protection against spring viremia of carp virus induced by a single-walled carbon nanotubes-based immersion DNA vaccine. Virology. 2019;537:216-25.
28. Kwak S-Y, Lew TTS, Sweeney CJ, Koman VB, Wong MH, Bohmert-Tatarev K, et al. Chloroplast-selective gene delivery and expression in planta using chitosan-complexed single-walled carbon nanotube carriers. Nature nanotechnology. 2019;14(5):447-55.
29. Pastorin G. Crucial functionalizations of carbon nanotubes for improved drug delivery: a valuable option? Pharmaceutical research. 2009;26(4):746.
30. Schneible JD, Young AT, Daniele M, Menegatti S. Chitosan Hydrogels for Synergistic Delivery of Chemotherapeutics to Triple Negative Breast Cancer Cells and Spheroids. Pharmaceutical Research. 2020;37(7):1-11.
31. Xia H, Jin H, Cheng Y, Cheng Z, Xu Y. The Controlled Release and Anti-Inflammatory Activity of a Tetramethylpyrazine-Loaded Thermosensitive Poloxamer Hydrogel. Pharmaceutical research. 2019;36(4):52.
32. Wang X-L, Yao H-F, Li X-Y, Wang X, Huang Y-P, Liu Z-S. pH/temperature-sensitive hydrogel-based molecularly imprinted polymers (hydroMIPs) for drug delivery by frontal polymerization. RSC advances. 2016;6(96):94038-47.
33. Sudre G, Siband E, Gallas B, Cousin F, Hourdet D, Tran Y. Responsive Adsorption of N-Isopropylacrylamide Based Copolymers on Polymer Brushes. Polymers. 2020;12(1):153.
34. De France KJ, Cranston ED, Hoare T. Mechanically Reinforced Injectable Hydrogels. ACS Applied Polymer Materials. 2020;2(3):1016-30.
35. Zhang N, Zheng S, Pan Z, Liu Z. Phase Transition Effects on Mechanical Properties of NIPA Hydrogel. Polymers. 2018;10(4):358.
36. Zhu J, Dou M, Lu M, Xiang X, Ding X, Liu W, et al. Thermo-responsive polymer grafted carbon nanotubes as the catalyst support for selective hydrogenation of cinnamaldehyde: Effects of surface chemistry on catalytic performance. Applied Catalysis A: General. 2019;575:11-9.
37. Kashani-Amin E, Sakhteman A, Larijani B, Ebrahim-Habibi A. Introducing a New Model of Sweet Taste Receptor, a Class C G-protein Coupled Receptor (C GPCR). Cell biochemistry and biophysics. 2019;77(3):227-43.
38. Alimohammadi E, Khedri M, Jahromi AM, Maleki R, Rezaian M. Graphene-Based Nanoparticles as Potential Treatment Options for Parkinson's Disease: A Molecular Dynamics Study. International Journal of Nanomedicine. 2020;15:6887.
39. Sahooli M, Sabbaghi S, Maleki R, Nematollahi M. Thermal conductivity of Water-based nanofluids: Prediction and comparison of models using machine learning. 2014.

534 40. Rezvantalab S, Moraveji M, Khedri M, Maleki R. An Insight into The Role of Riboflavin Ligand on
535 the Self-assembly of Poly (lactic-co-glycolic acid)-based Nanoparticles, A Molecular Simulation and
536 Experimental Approach. Soft Matter. 2020.
537 41. Maleki R, Khoshoei A, Ghasemy E, Rashidi A. Molecular insight into the smart functionalized
538 TMC-Fullerene nanocarrier in the pH-responsive adsorption and release of anti-cancer drugs. Journal of
539 Molecular Graphics and Modelling. 2020;100:107660.
540 42. Mahdavi M, Fattahi A, Tajkhorshid E, Nouranian S. Molecular Insights into the Loading and
541 Dynamics of Doxorubicin on PEGylated Graphene Oxide Nanocarriers. ACS Applied Bio Materials. 2020.
542 43. Contreras ML, Torres C, Villarroel I, Rozas R. Molecular dynamics assessment of doxorubicin–
543 carbon nanotubes molecular interactions for the design of drug delivery systems. Structural Chemistry.
544 2019;30(1):369-84.
545 44. Khoshoei A, Ghasemy E, Poustchi F, Shahbazi M-A, Maleki R. Engineering the pH-sensitivity of
546 the graphene and carbon nanotube based nanomedicines in smart cancer therapy by grafting trimetyl
547 Chitosan. Pharmaceutical Research. 2020;37(8):1-13.

548

Figures

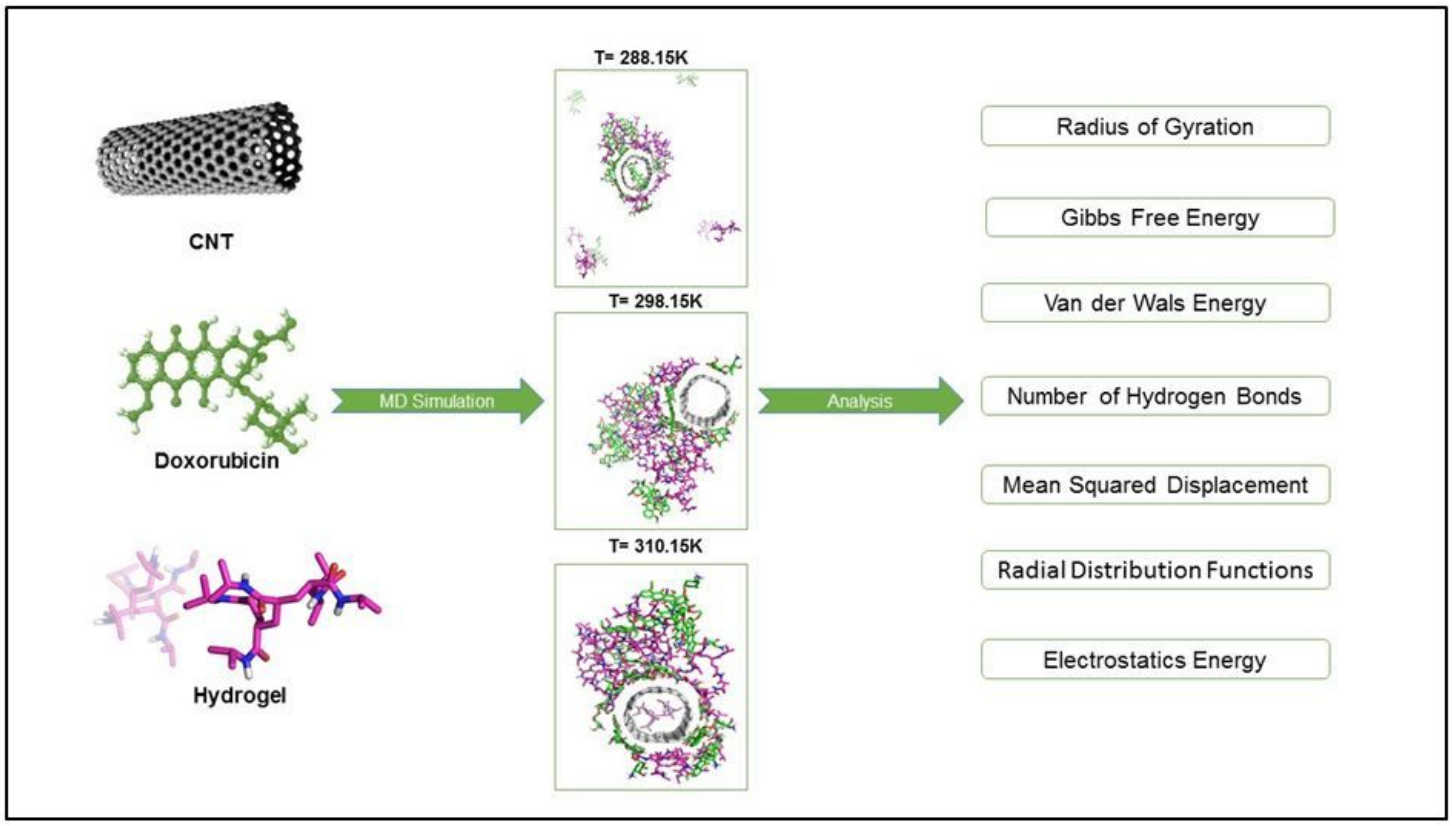

Figure 1

Flow Chart

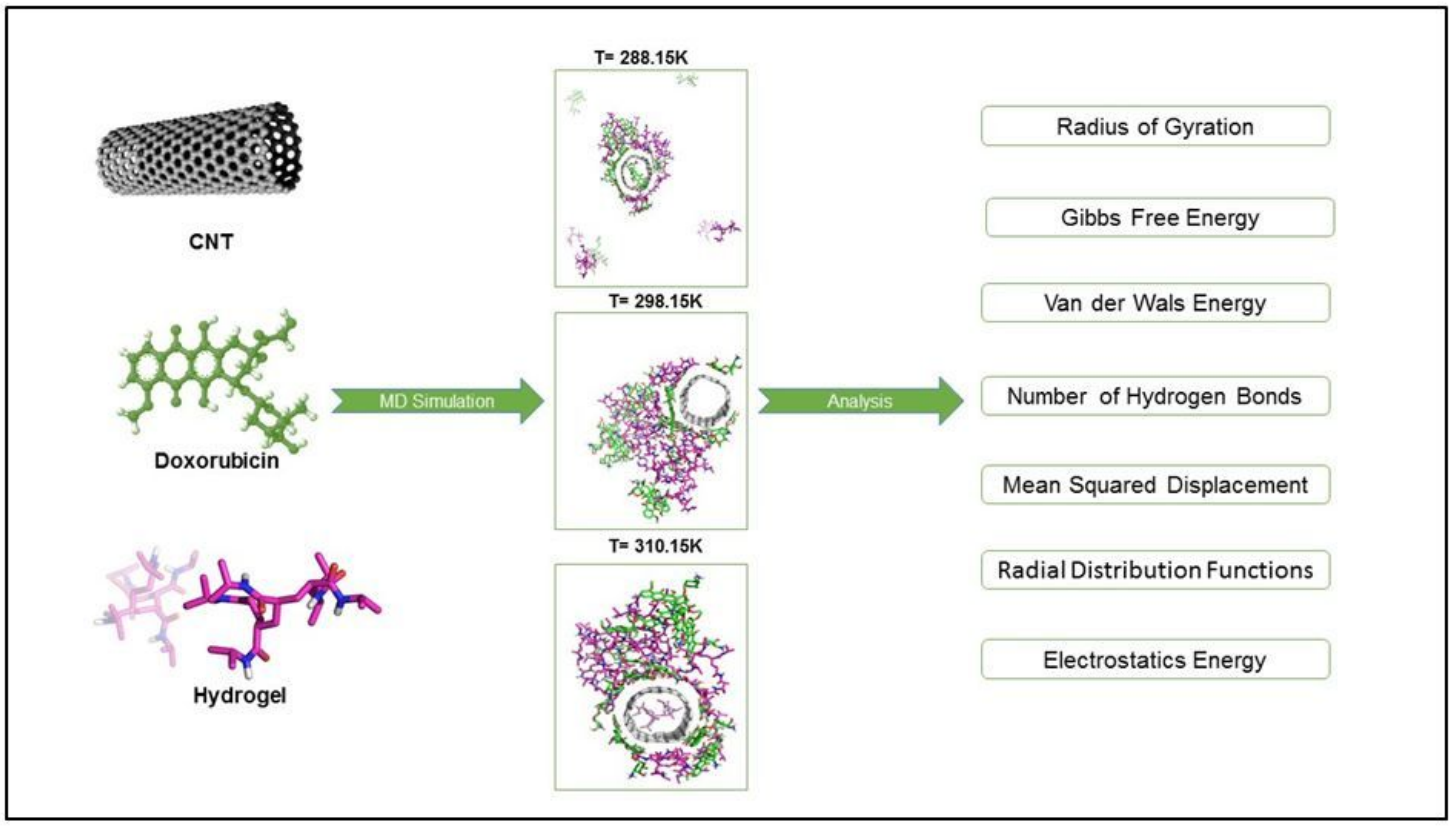

Figure 1

Flow Chart

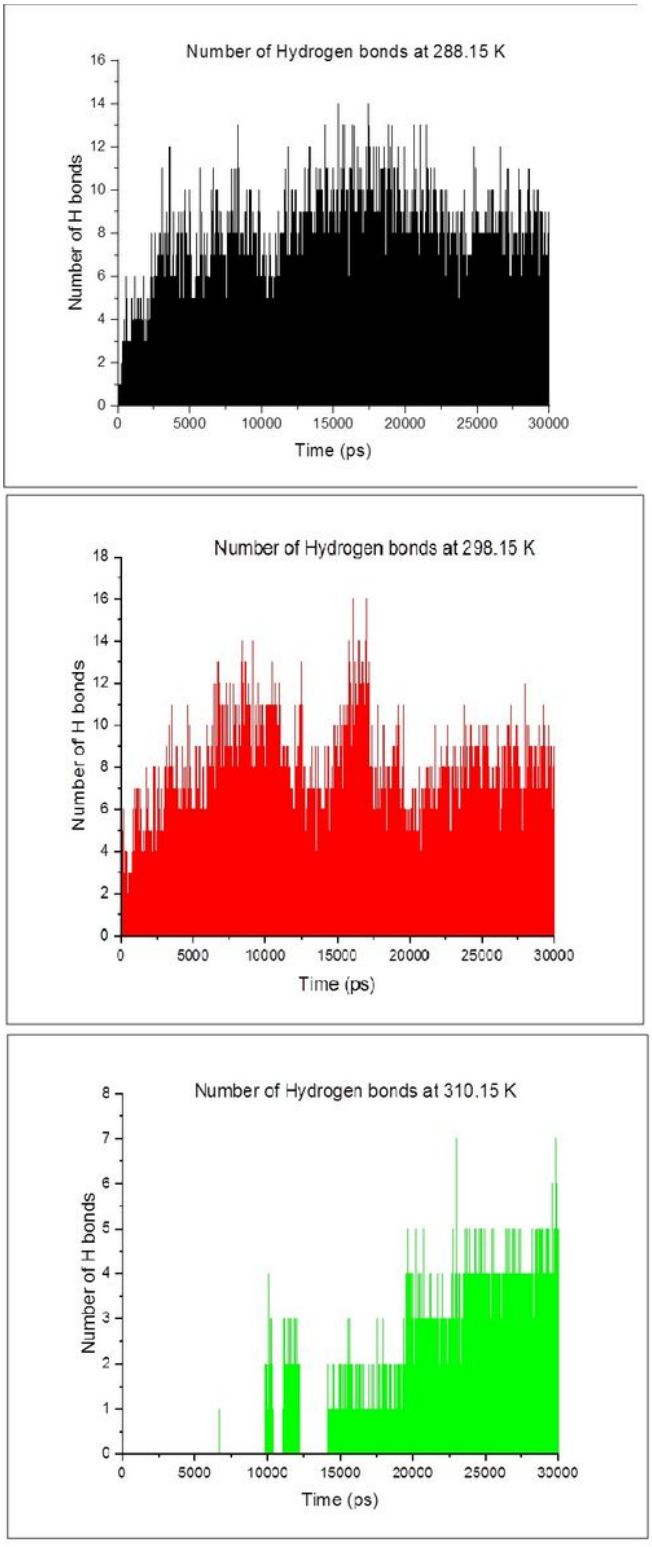

Figure 2

The numbers of hydrogen bonds between DOX and NIPA at three different temperatures

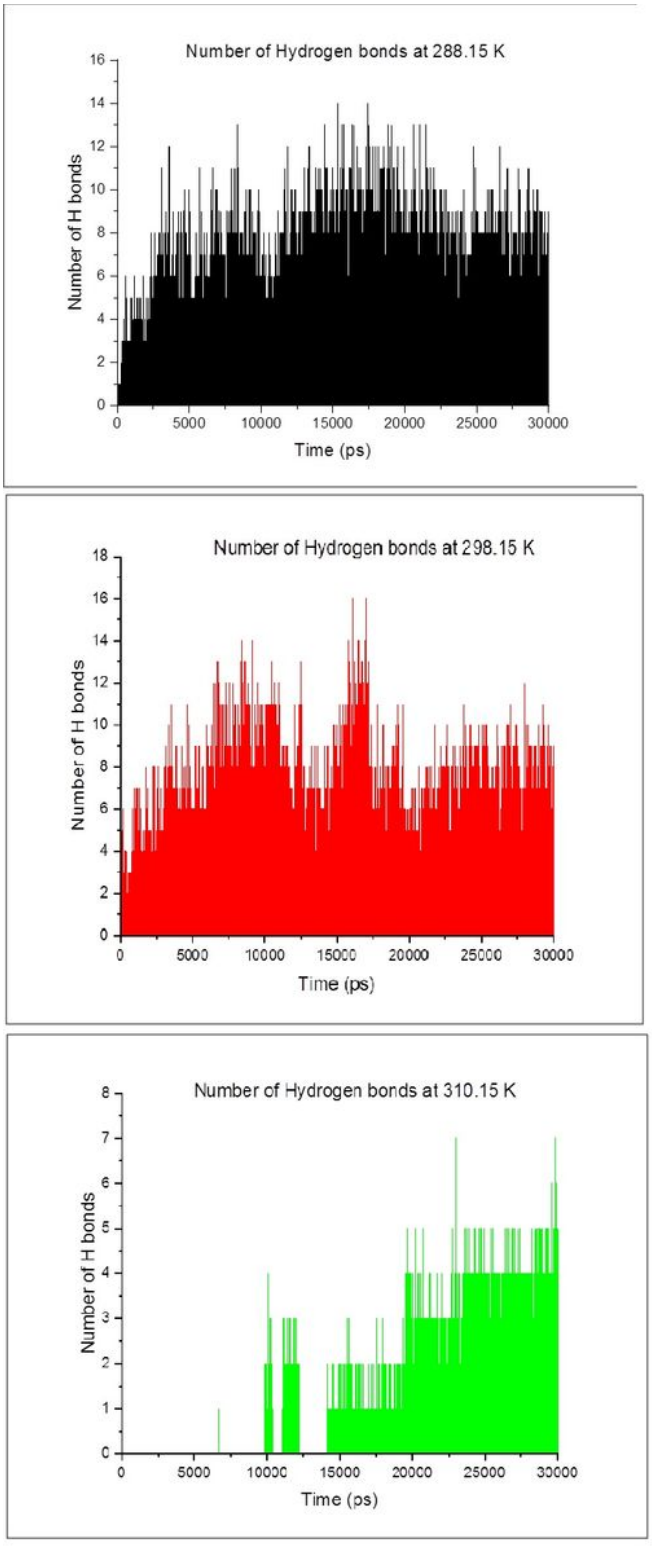

Figure 2

The numbers of hydrogen bonds between DOX and NIPA at three different temperatures

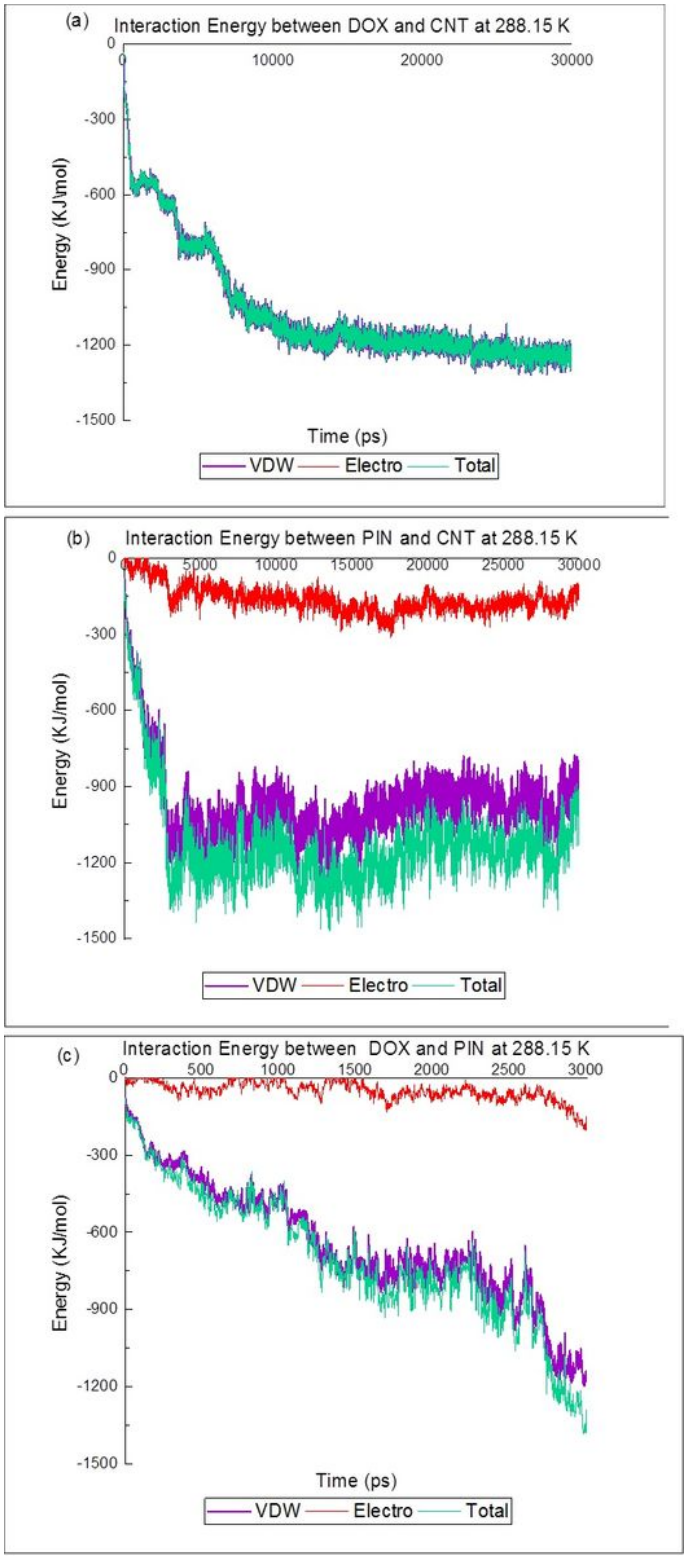

Figure 3

Interaction energies diagrams at 288.15 K (a) Electrostatic and van der Waals energies of DOX@CNT interaction versus time at 288.15 K; (b) Electrostatic and van der Waals energies of NIPA@CNT interaction versus time at 288.15 K; (c) Electrostatic and van der Waals energies of DOX@NIPA interaction versus time in 288.15 K

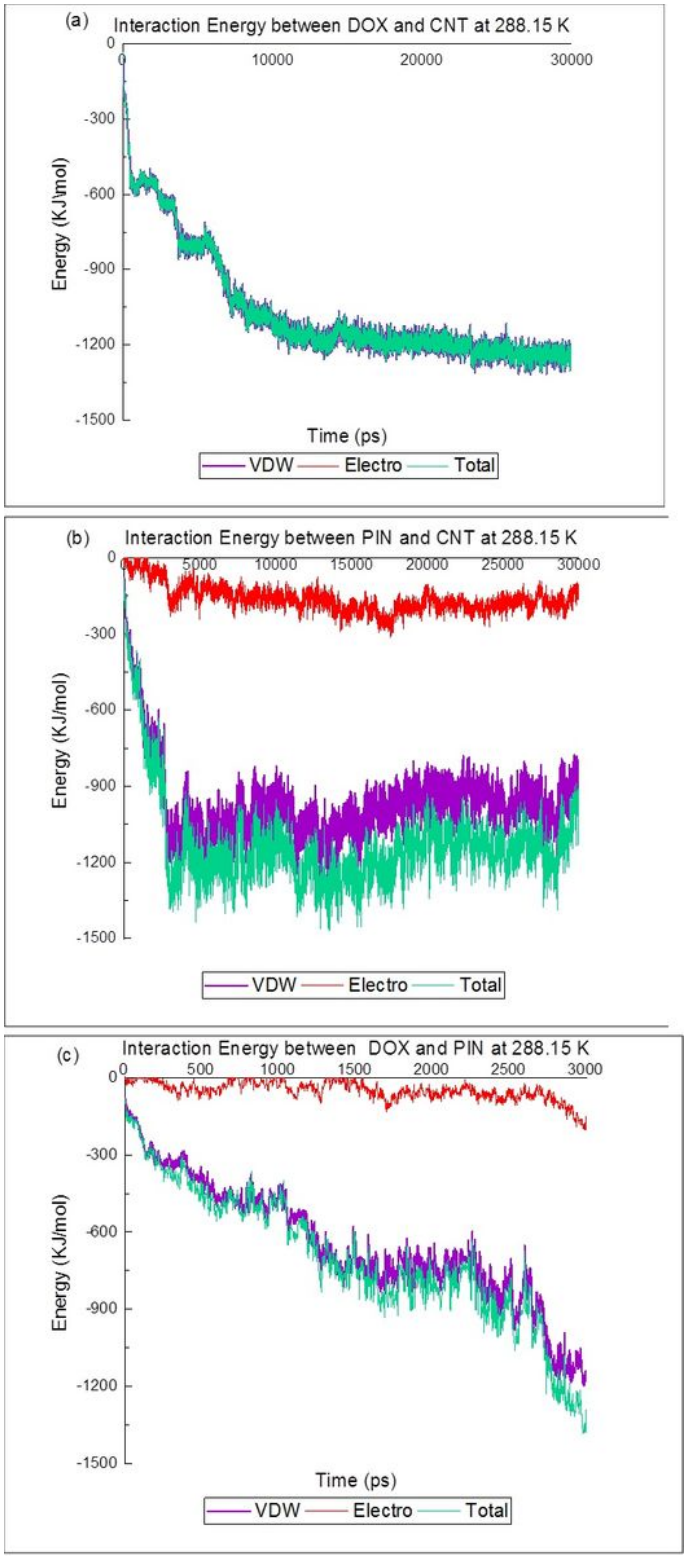

Figure 3

Interaction energies diagrams at 288.15 K (a) Electrostatic and van der Waals energies of DOX@CNT interaction versus time at 288.15 K; (b) Electrostatic and van der Waals energies of NIPA@CNT interaction versus time at 288.15 K; (c) Electrostatic and van der Waals energies of DOX@NIPA interaction versus time in 288.15 K

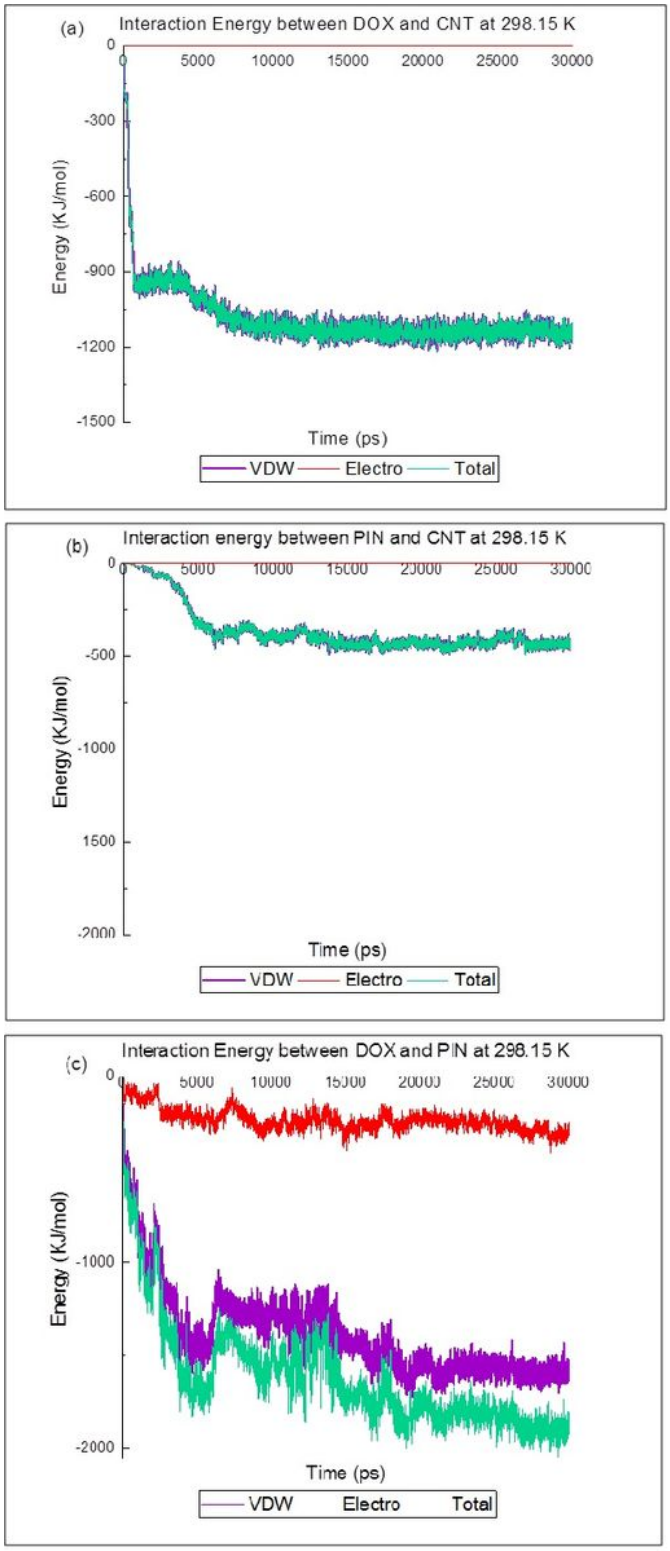

Figure 4

Interaction energies diagrams at 298.15 K (a) Electrostatic and van der Waals energies of DOX@CNT interaction versus time at 298.15 K; (b) Electrostatic and van der Waals energies of NIPA@CNT interaction versus time at 298.15 K; (c) Electrostatic and van der Waals energies of DOX@NIPA interaction versus time in 298.15 K.

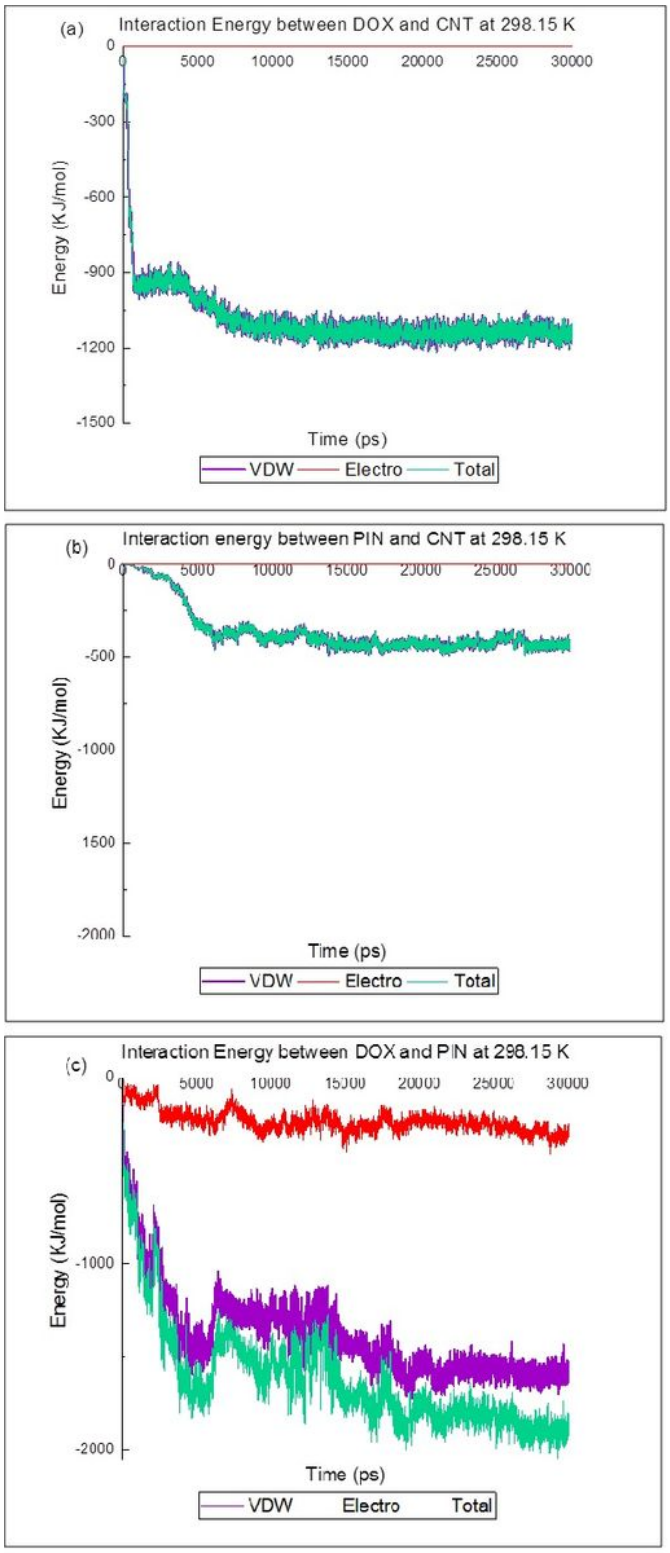

Figure 4

Interaction energies diagrams at 298.15 K (a) Electrostatic and van der Waals energies of DOX@CNT interaction versus time at 298.15 K; (b) Electrostatic and van der Waals energies of NIPA@CNT interaction versus time at 298.15 K; (c) Electrostatic and van der Waals energies of DOX@NIPA interaction versus time in 298.15 K.

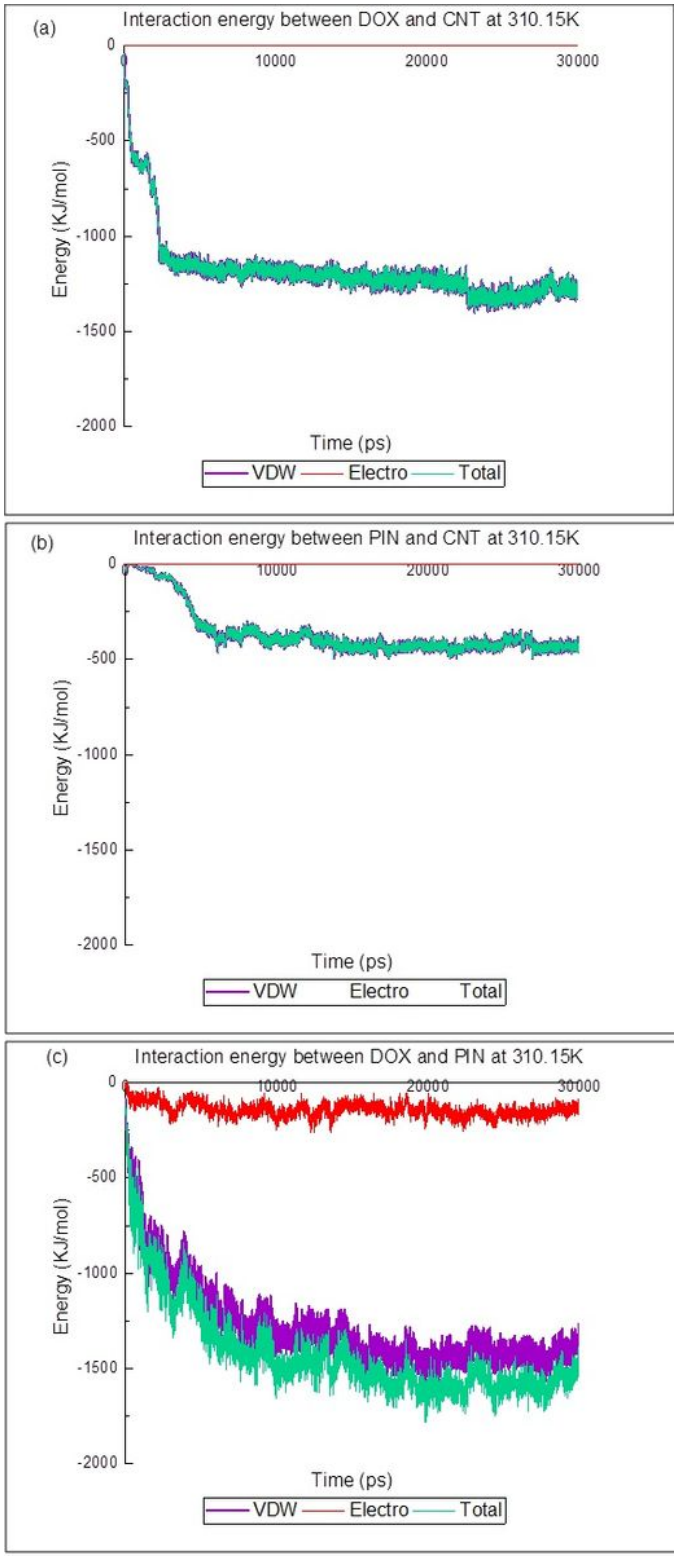

Figure 5

Interaction energies diagrams at 310.15 K (a) Electrostatic and van der Waals energies of DOX@CNT interaction versus time at 310.15 K; (b) Electrostatic and van der Waals energies of NIPA@CNT interaction versus time at 310.15 K (c) Electrostatic and van der Waals energies of DOX@NIPA interaction versus time in 310.15 K.

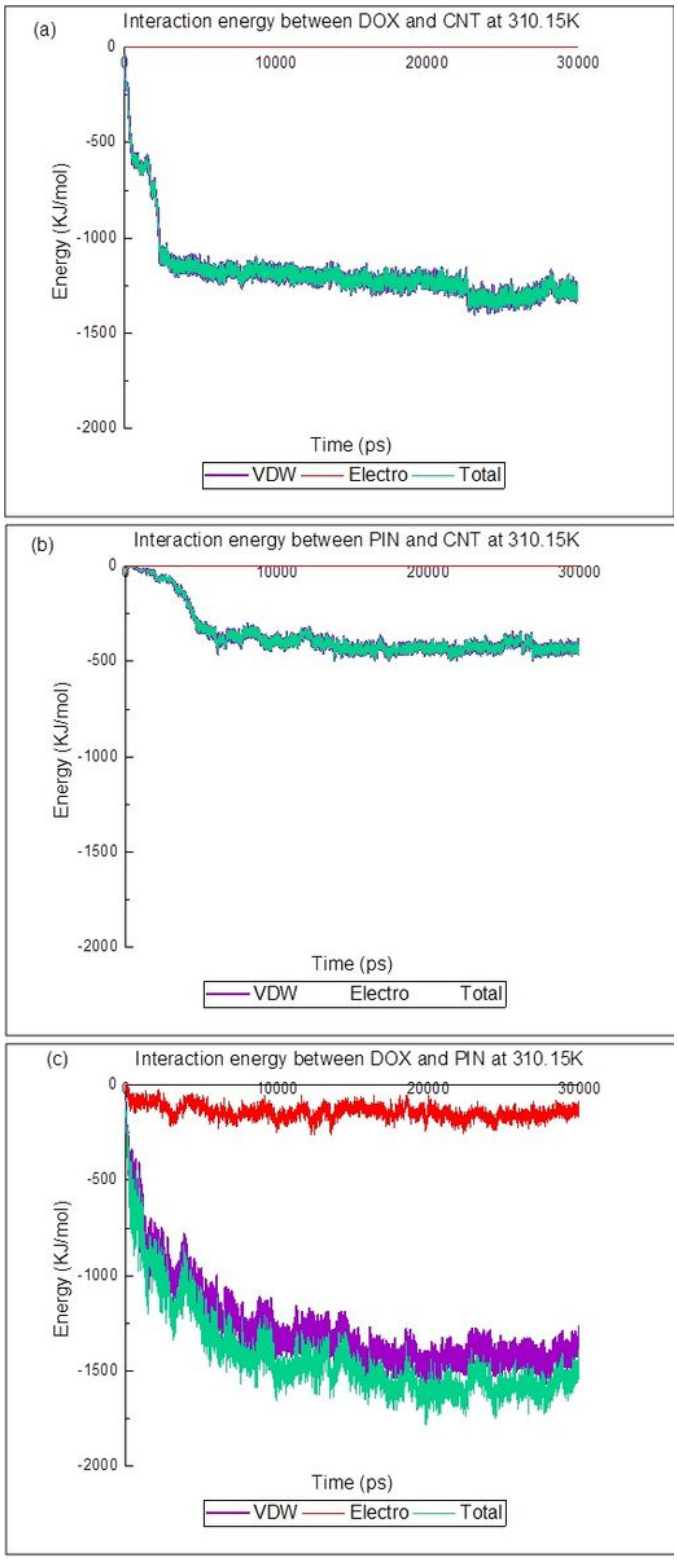

Figure 5

Interaction energies diagrams at 310.15 K (a) Electrostatic and van der Waals energies of DOX@CNT interaction versus time at 310.15 K; (b) Electrostatic and van der Waals energies of NIPA@CNT interaction versus time at 310.15 K (c) Electrostatic and van der Waals energies of DOX@NIPA interaction versus time in 310.15 K.

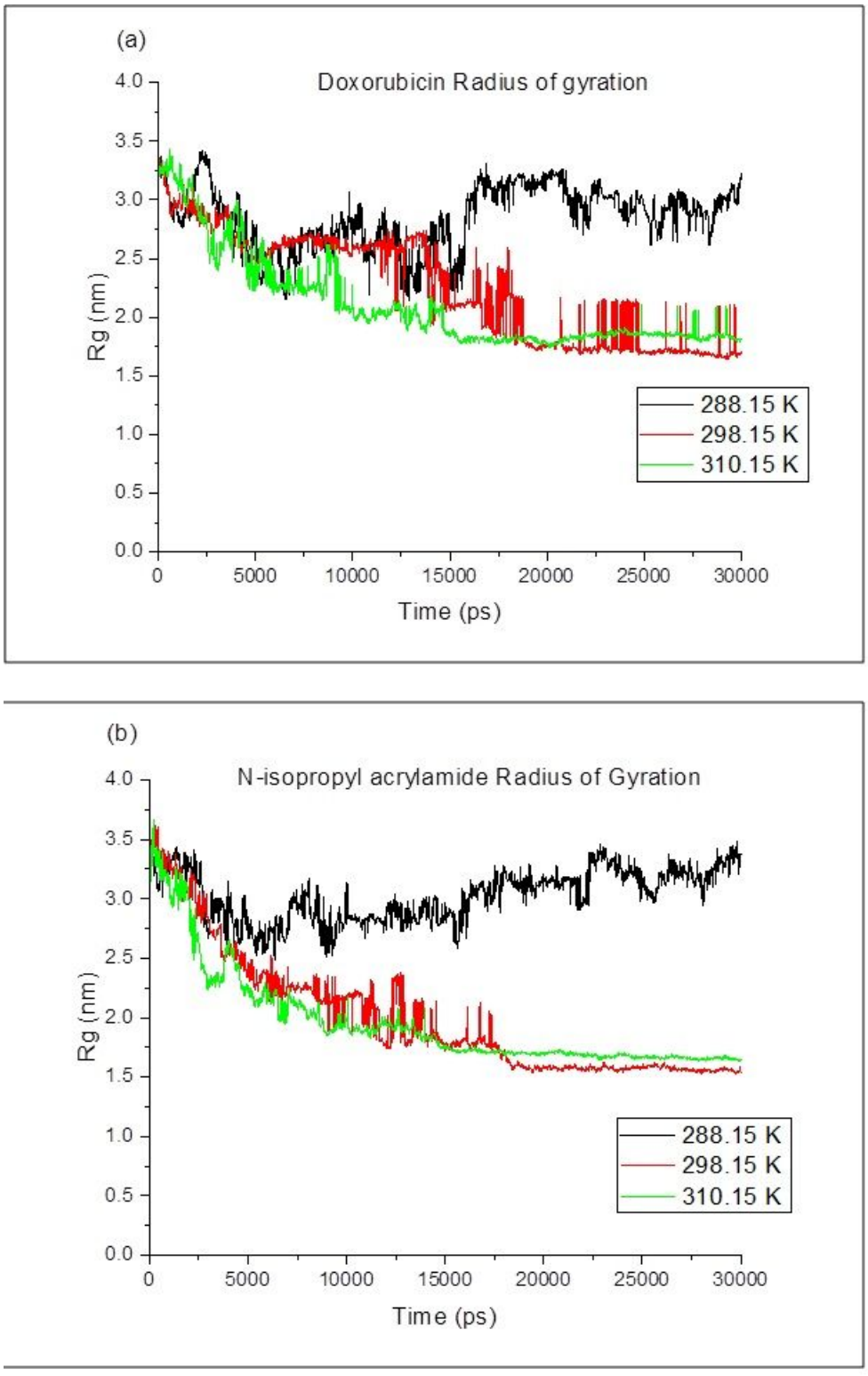

Figure 6

Gyration Radius of Molecules versus time in different temperatures for CNT carrier: (a) DOX Rg at three temperatures (b) NIPA Rg at three temperatures

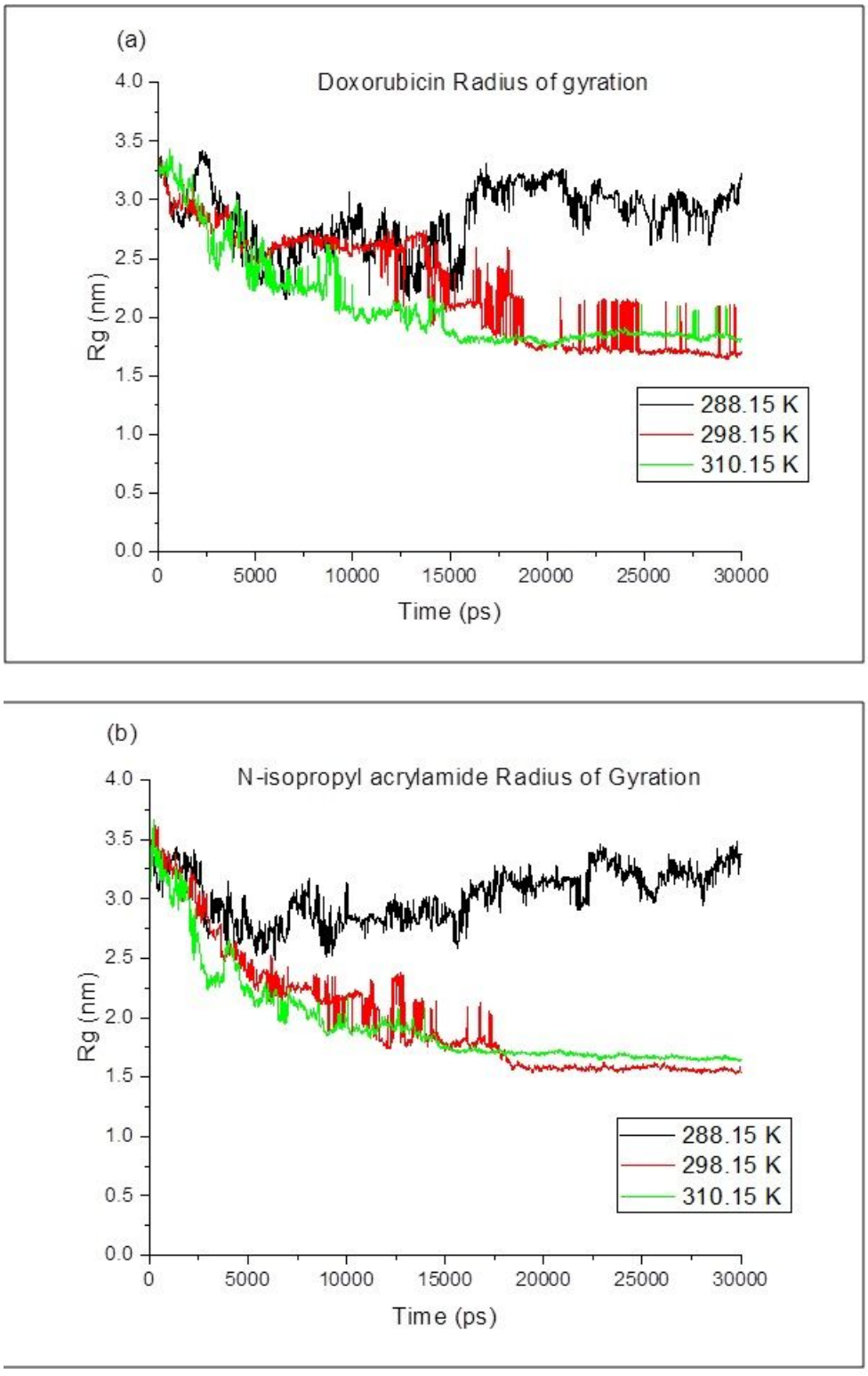

Figure 6

Gyration Radius of Molecules versus time in different temperatures for CNT carrier: (a) DOX Rg at three temperatures (b) NIPA Rg at three temperatures

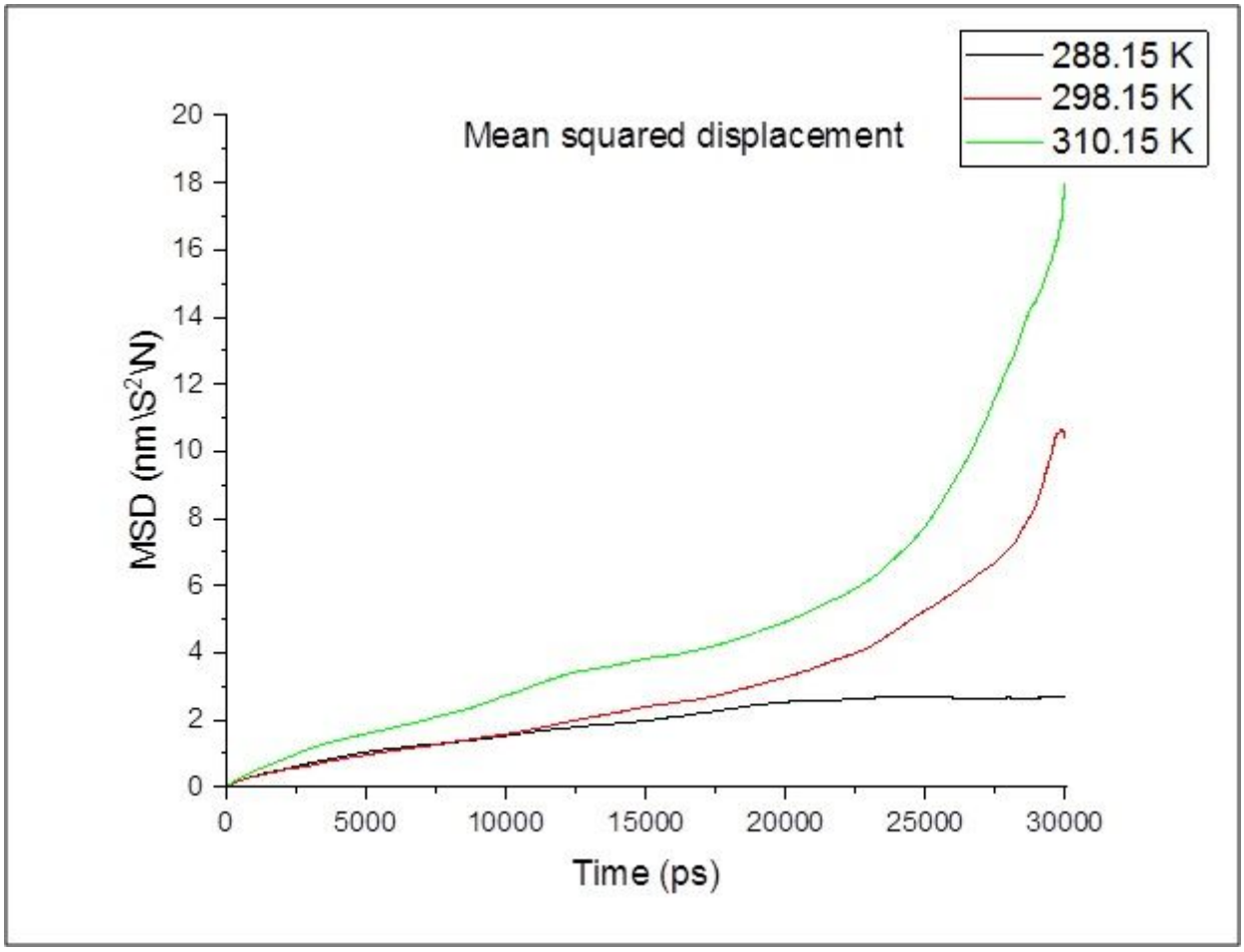

Figure 7

Mean square displacement of the system versus time at different temperature

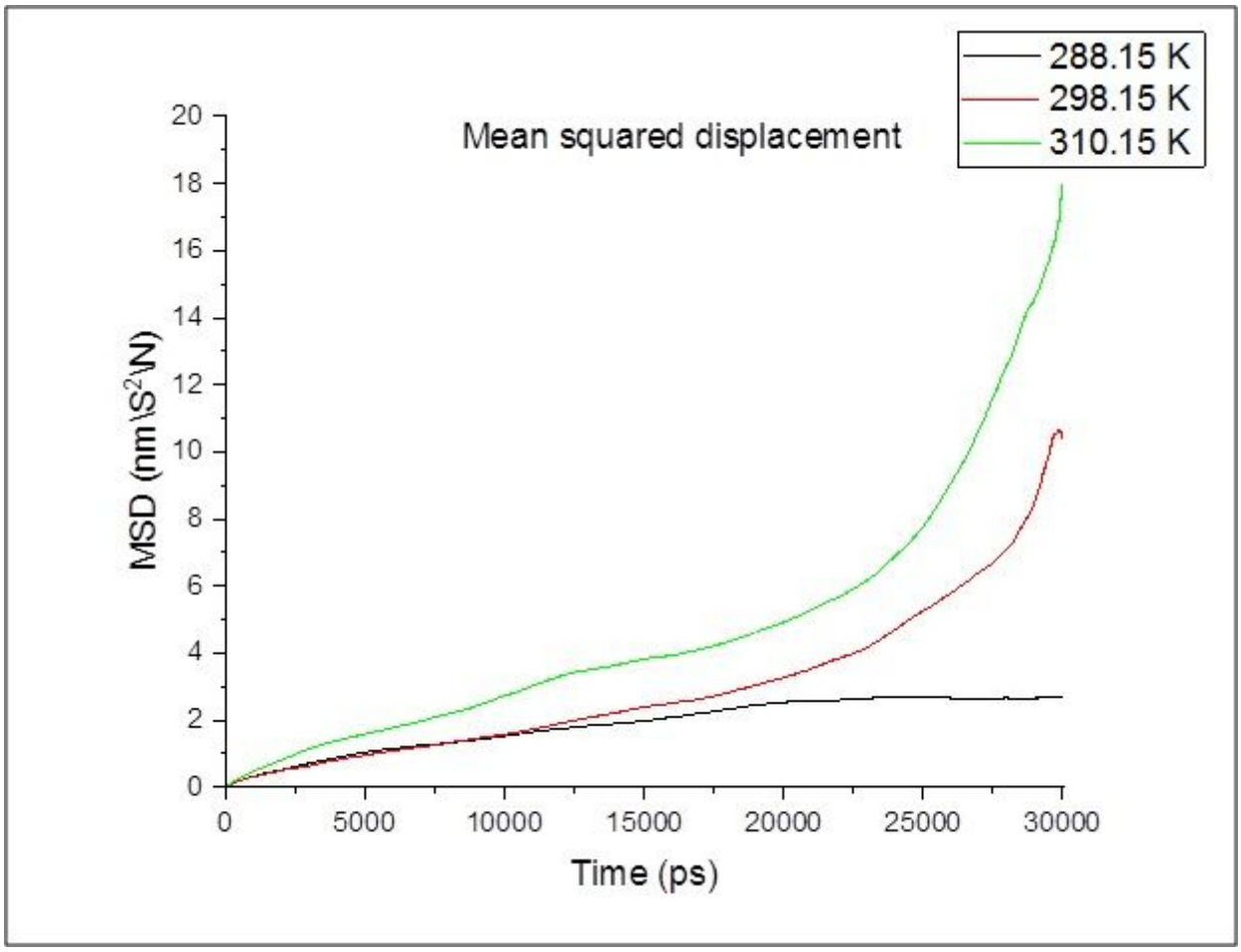

Figure 7

Mean square displacement of the system versus time at different temperature

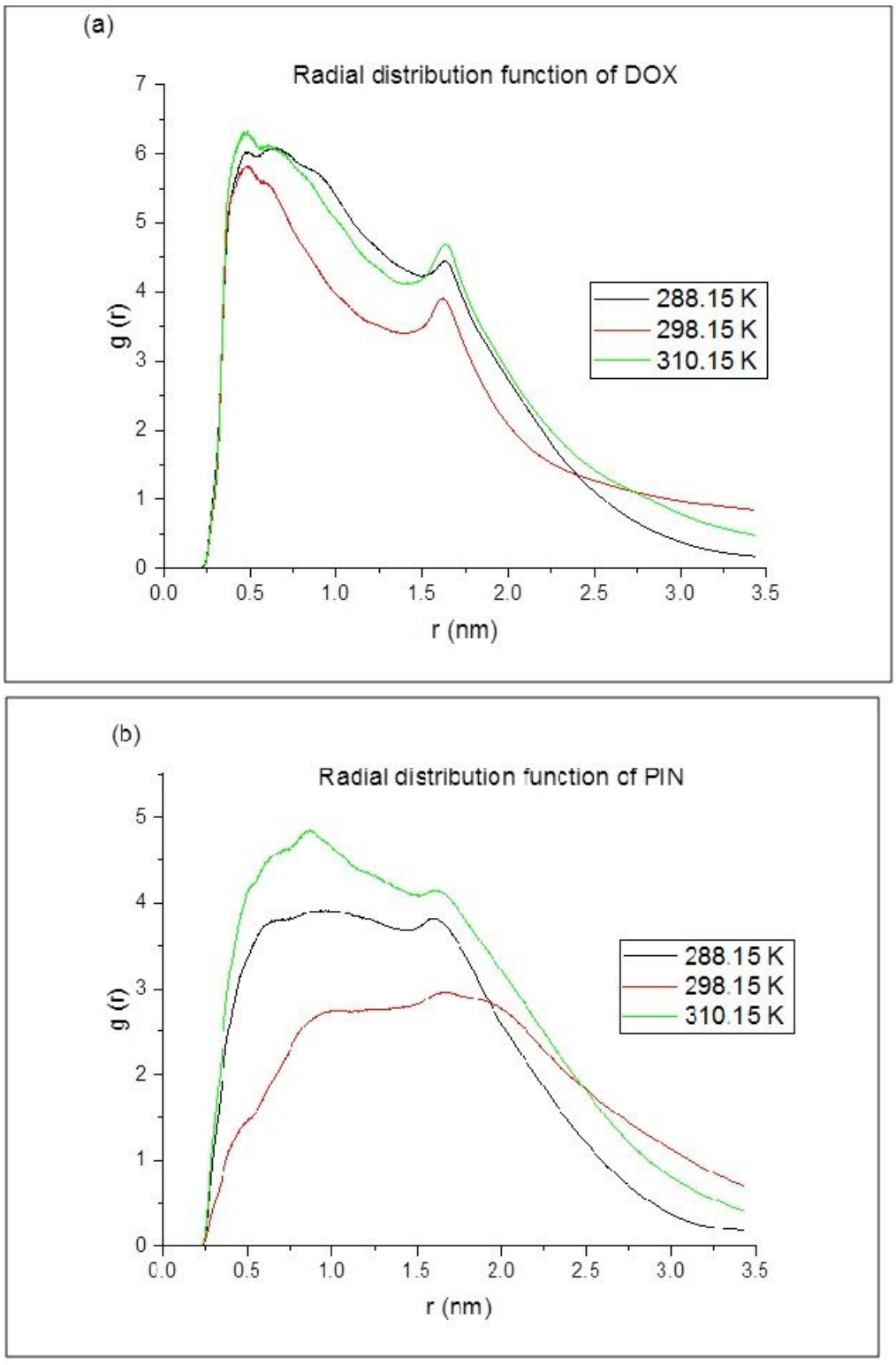

Figure 8

The radial distribution function of the DOX@CNT and NIPA@CNT versus location at different temperatures: (a) The RDF of the DOX at three temperatures; and (b) the RDF of the NIPA at three temperatures.

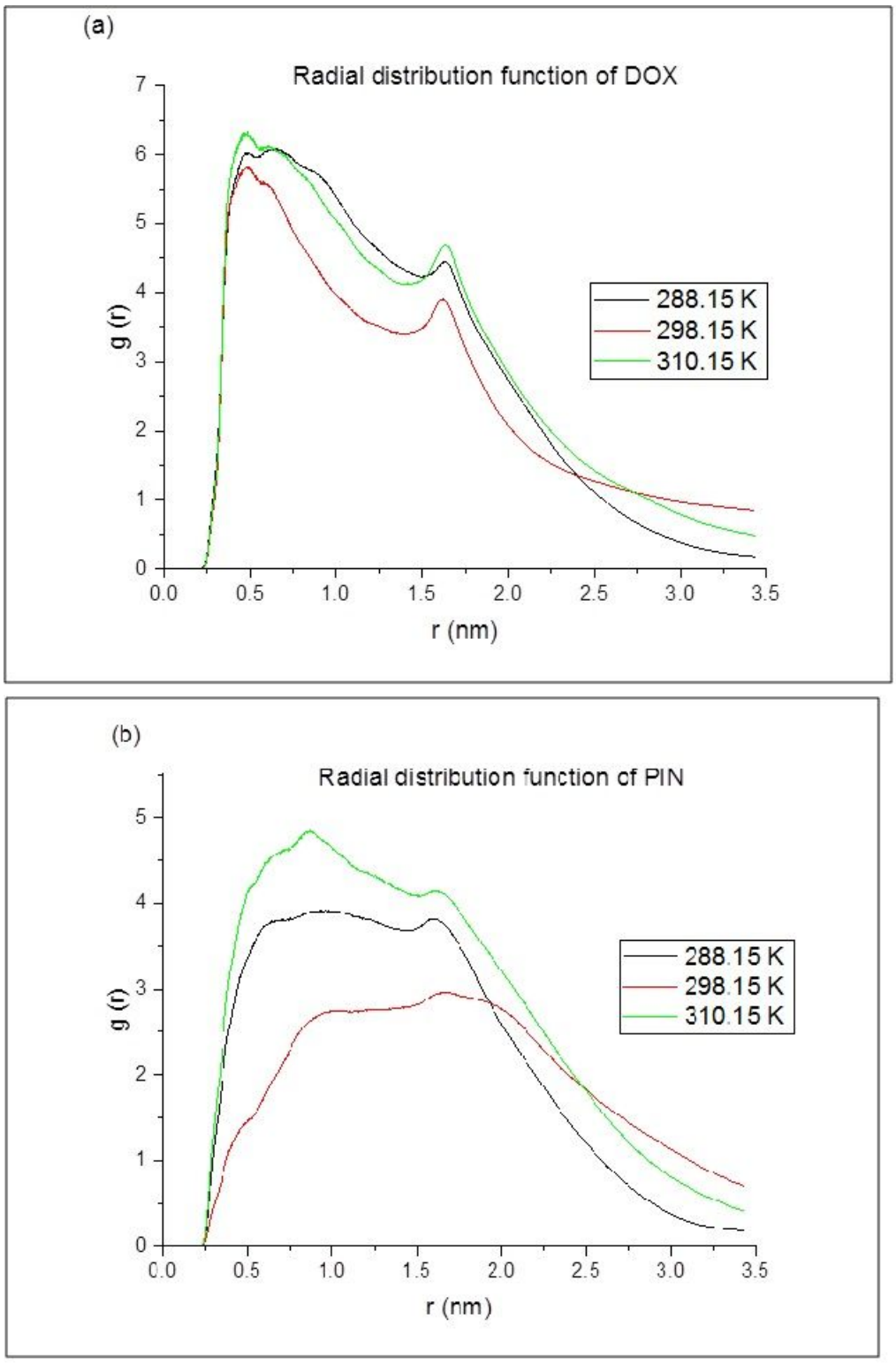

Figure 8

The radial distribution function of the DOX@CNT and NIPA@CNT versus location at different temperatures: (a) The RDF of the DOX at three temperatures; and (b) the RDF of the NIPA at three temperatures.

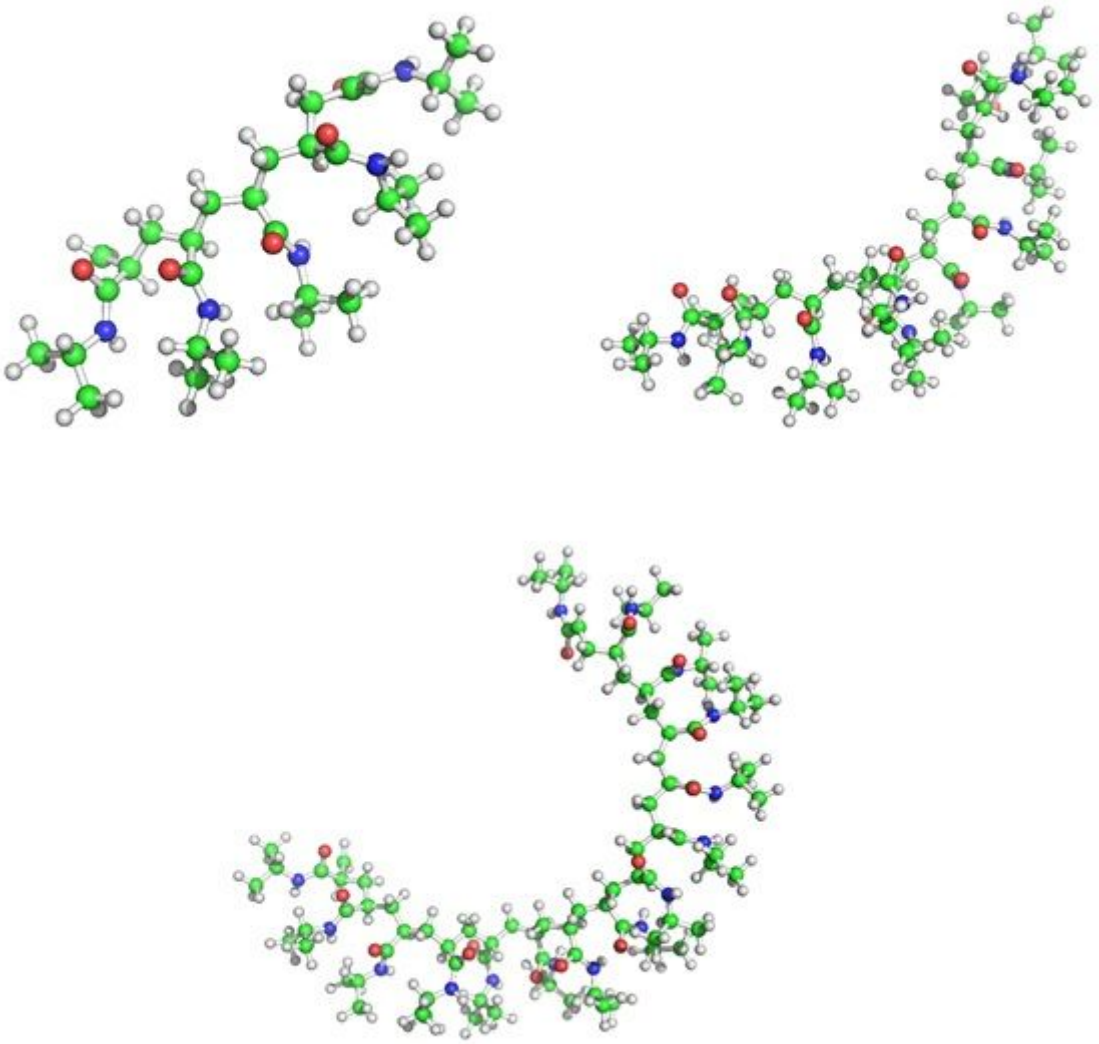

Figure 9

The 3D image of the 5-mer, 10-mer, and 15-mer polymer

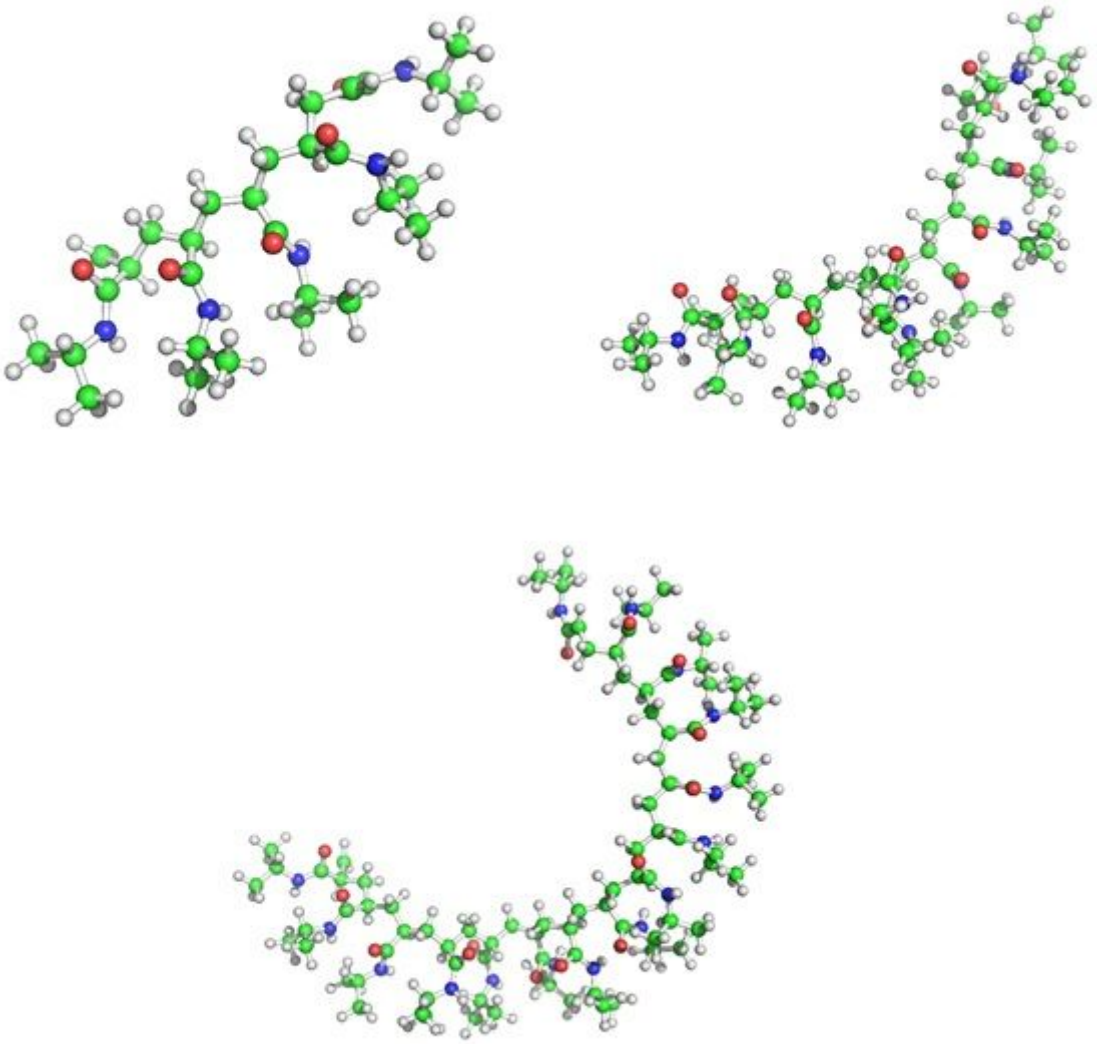

Figure 9

The 3D image of the 5-mer, 10-mer, and 15-mer polymer